HYDROGEN - OXYGEN HIGH P_c APS ENGINES

Report 14354-Q-4 14 July 1971

Quarterly Report for Period Ending 1 July 1971

by

L. Schoenman

Engine Components Department
Aerojet Liquid Rocket Company
Sacramento, California

for

NATIONAL AERONAUTICS AND SPACE ADMINISTRATION
Lewis Research Center
Cleveland, Ohio 44135

FOREWORD

This is the fourth quarterly report for Contract NAS 3-14354. The purpose of this contract is the development of a comprehensive technology base for high performance, long life, gaseous hydrogen-gaseous oxygen rocket engines suitable for the Space Shuttle APS. Significant goals in thruster design are a 50-hour firing life over a 10-year period, with up to 10^6 restarts, and single firings up to 1000 sec.

The program was initially structured as two parallel efforts: one directed toward high pressure (100 to 500 psia) systems and the other toward low pressure (10 to 20 psia) systems. Nominal engine thrust in each case is 1500 lb. Initial program tasks were devoted to the analytical evaluation and screening of injector and cooled thrust chamber concepts for both pressure levels. This was followed by closely paralleled but separate experimental evaluations of low and high pressure injectors and ignition devices. Recommendations of specific injector and igniter designs have been made for both pressure levels as a result of these tests.

As these parallel efforts were about to enter the cooled chamber fabrication phase, the program was redirected to apply additional emphasis on the high P_c technology with a revised schedule on propellant inlet temperatures. Activities on the low pressure phase were terminated by a stop work order, which eliminated the requirements for a portion of the injector testing and all of the low P_c cooled chamber fabrication, durability and pulse testing. The program's resources originally planned for these activities have been reallocated to expand design and test efforts related to the lower temperature gaseous propellants. The high P_c technology effort is now in the full 40:1 nozzle/thrust chamber assembly test phase.

Mr. L. Schoenman, project manager for the high pressure phase, reports to Dr. R. J. LaBotz, who is program manager of all ALRC APS thruster programs. The NASA Lewis Research Center program manager is Mr. J. Gregory.

TABLE OF CONTENTS

TABLE LIST

FIGURE LIST

FIGURE LIST (cont.)

I. PROGRAM OBJECTIVES

The primary objective of this contract is to generate a comprehensive technology base for high performance gaseous hydrogen-gaseous oxygen rocket engines suitable for the Space Shuttle Auxiliary Propulsion System (APS). Durability requirements include injector and thrust chamber designs capable of 50 hours of firing life over a 10-year period with up to 10^6 pulses and single firings up to 1000 sec. These technical objectives are being accomplished and reported upon in a 28-task program summarized below. The first ten tasks relate to high pressure APS engines; parallel Tasks XI through XX relate to low pressure APS engines, and Task XXI is a common reporting task. The additional tasks are for the expanded High P_c Low Temperature Program.

	High P_c Task		
Task Titles	Ambient Propellant	Low Temp Propellant	Low P_c Task
Injector analysis and design	I*	XXII	XI*
Injector fabrication	II*	XXIII	XII*
Thrust chamber analysis and design	III*	XXIV	XIII*
Thrust chamber fabrication	IV	XXV	XIV*
Ignition system analysis and design	V*	--	XV*
Ignition system fabrication and checkout	VI*	--	XVI*
Propellant valves preparation	VII*	--	XVII*
Injector tests	VIII*	XXVI	XVIII*
Thrust chamber cooling tests	IX	XXVII	XIX*
Pulsing tests	X	XXVIII	XX*
	Common Task		
Reporting requirements	XXI		

*Completed tasks for revised program.

II. SUMMARY OF ACCOMPLISHMENTS

At the conclusion of the report quarter, the first eight High P_c program tasks had been completed and Task IX, testing of 40:1 area ratio cooled chambers, initiated. All activities related to the Low P_c thrusters were terminated and substantial progress has been made in reoptimization of High P_c components for low temperature propellants.

Significant High P_c program milestones were:

(1) Completion of cooled chamber fabrication (two film-cooled and two regeneratively cooled thrusters).

(2) Eleven restarts of the first 40:1 film-cooled chamber for an accumulated 655 sec of firing. The longest single test was 278 sec.

(3) Demonstration of a wide range of operating conditions:

Chamber pressure	100 to 500 psia
Propellant temperature	200 to 600°R
Mixture ratio	3 to 5
Film cooling flows	30 to 19%

(4) Achievement of performance goals of 435 sec I_s at 22% fuel film cooling.

(5) Long duration firings with an injector which has been restarted over 2600 times.

(6) Smooth, reliable chamber ignitions in all tests at vacuum conditions.

(7) Completion of fabrication of the first new injector optimized for low temperature propellants.

III. PROGRESS BY TASK

A. ACTIVITIES FOR AMBIENT TEMPERATURE PROPELLANTS

1. Tasks I Through III - No activities of significance.

2. Task IV - Cooled Chamber Fabrication

a. Hardware Status

The status of the four cooled 40:1 chambers at the close of this report is as follows:

Film-Cooled Chambers (Figure 1)

SN 1 - Fabrication and instrumentation complete. Thrust chamber on J-3 test stand. Fired 11 times for a total duration of 655 sec.

SN 2 - Fabrication complete; leak and coolant channel cold flow satisfactory. Instrumentation complete. Skirt insulation in progress.

Regeneratively Cooled Chambers (Figure 2)

SN 1 - Fabrication complete; leak check and cold flow complete. Instrumentation and skirt insulation complete. Chamber in J-Area awaiting testing.

SN 2 - Fabrication complete. Unit is being returned from Electroforms Inc., where nickel pressure case was deposited. Leak check, cold flow, and instrumentation remain to be completed.

(A)

(B)

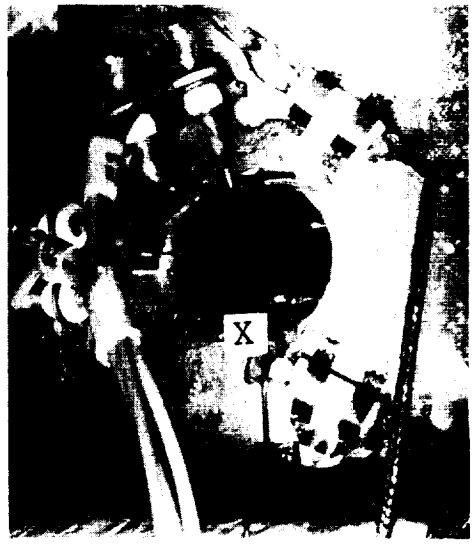

X Gas-Side and Backside Temperature Measurement

(C)

(A) Instrumentation in process
(B) Instrumentation and skirt insulation complete
(C) Thermocouple and strain patch detail

Figure 1. Film-Cooled Thrust Chamber

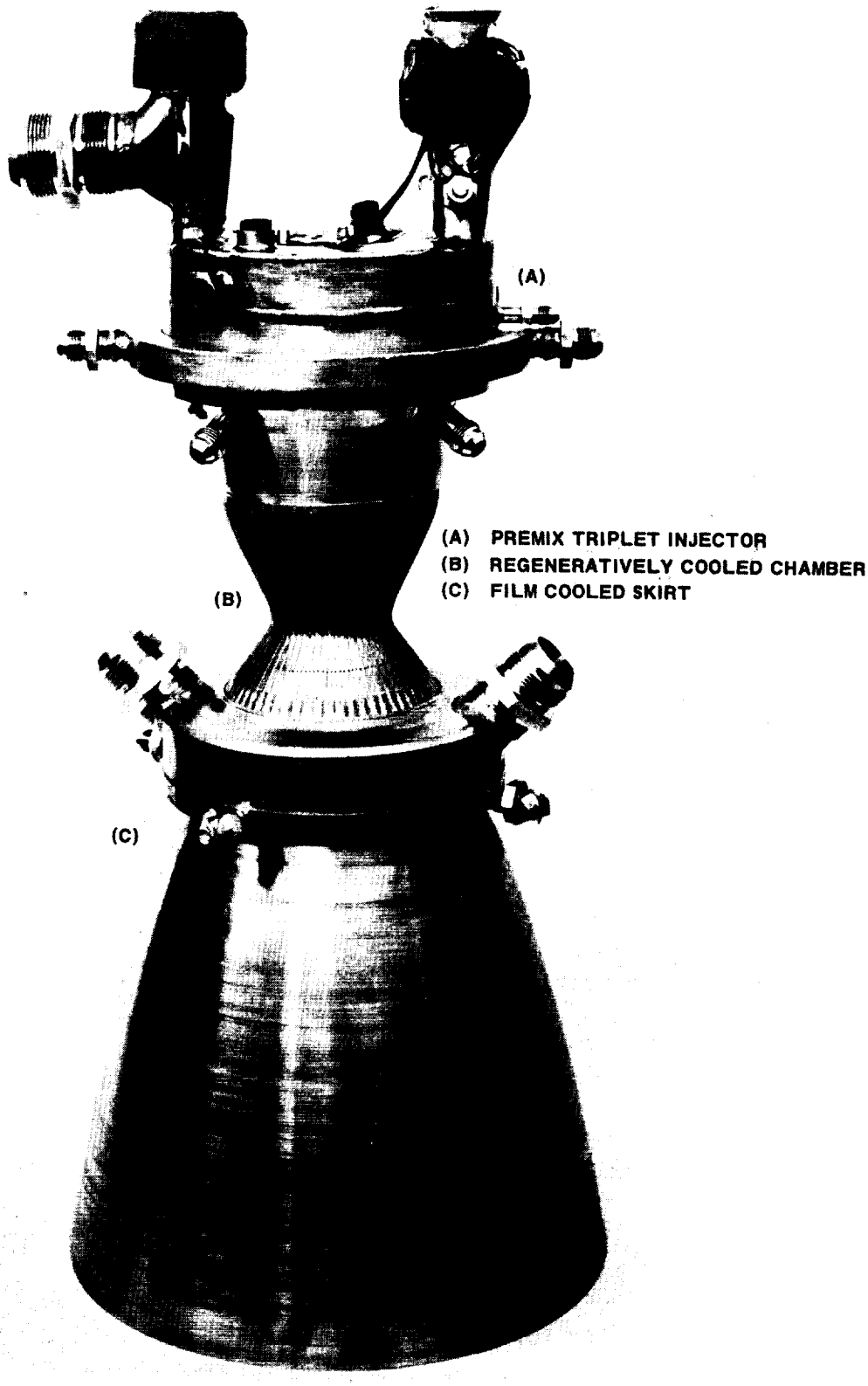

Figure 2. Regeneratively Cooled Thrust Chamber Prior to Electroforming Jacket and Instrumentation

III, A, Activities for Ambient Temperature Propellants (cont.)

b. Fabrication Task Summary

The 40:1 cooled thrust chambers designed and fabricated under this task employed proven state-of-the-art fabrication methods. Fabrication of these chambers has proceeded, to date, without encountering major fabrication difficulties. Minor problems periodically encountered were resolved and all components completed are of a quality which is acceptable for this technology program.

The spinning of stainless steel skirts to the Rao nozzle contour was proven to be a simple, low cost operation which is most applicable to quantity production. The same is true of the use of photoetched nozzles for the supersonic film cooling injection ring. The spinning operations on the Haynes 188 throat sections from conical rolled and welded preforms proved somewhat more difficult and time consuming because of the need for frequent heat treatment and descaling operations. Slight modifications to the conical preforms for future parts would greatly reduce the number of heat treatment cycles and make the component suitable for low-cost quantity production.

Initial difficulties in cutting deep, narrow slots in the regeneratively cooled copper chamber were a result of using non-optimum tooling and cutting rates. Slotting operations proceeded smoothly once proper cutters were obtained and feed rates established. All designs employ constant width cooling channels and are free of splits or bifurcations. Components containing cooling channels, therefore, also lend themselves to low-cost quantity production.

The two approaches to coolant channel closeout employed were (1) shrink fit the copper liner containing the coolant channels into a thin wall (0.060 in.) steel jacket for the film-cooled design, and (2) braze rectangular wires into a stepped coolant slot for the regeneratively cooled chamber design.

III, A, Activities for Ambient Temperature Propellants (cont.)

In the latter approach, the initial channel is cut with a 0.060-in.-wide cutter and 0.060-in. constant depth. A second variable depth, 0.050-in.-wide contour cut formed the coolant channels of variable cross-sectional flow area. Channel closeout was accomplished by brazing precontoured 0.060-in. square copper wires into the slots. The 0.005-in. ledge formed by the stepped machining provides a positive channel depth control.

Braze assembly of components was conducted on a one-chamber-at-a-time schedule. In some instances, it was necessary to repeat a braze run to obtain proper flow of braze material and to install gas-side thermocouples or flanges. The ability to recycle components at or after the final assembly stage is a desirable feature.

The pressure vessel structure in the regeneratively cooled design (hoop loading cannot be carried by copper wires at 500 psia chamber pressure) is provided by electroforming a thin nickel jacket over the chamber following the wire braze. The electroformed nickel is isolated from the hydrogen by the wire closeout and therefore not subject to the embrittlement phenomena associated with the electroformed material.

The shrink fit and braze approach to closure employed on the film-cooled design has proven to be simpler and less time consuming than the square wire braze and nickel electroform. This approach has the following advantages: (a) the expansion coefficient of copper and stainless steel is nearly identical as compared to 2×10^{-6} in./in.-°F differential between copper and nickel, and (b) the steel/copper assembly can be rebrazed to permit installation of gas-side thermocouples. Limitations inherent in the electroforming closure are the inability to braze in gas-side thermocouples following electroforming due to potential blistering of the electroformed surface. When thermocouples are brazed prior to electroforming, it becomes impractical to finish machine the rough exterior surface. Additional

III, A, Activities for Ambient Temperature Propellants (cont.)

undesirable tendencies noted on the first chamber assembly include nonuniform material deposition in both the circumferential as well as axial directions and some minor chamber warpage. A modification to the electroforming procedure was being evaluated for the second chamber assembly to determine if some of these shortcomings can be overcome. These results are still being evaluated.

c. Chamber Acceptance Tests

In addition to normal leak and pressure tests, each finished chamber is cold flowed with GN_2 to determine: (a) chamber flow coefficient, and (b) flow uniformity within the coolant channels and to detect possible plugged channels. Figure 3 shows the coolant channel flow distribution in SN 2 film-cooled chamber using a single inlet to feed a constant area manifold. Flow distribution falls within $\pm$10% of the nominal values with the exception of several channels located on either side of the inlet line. The low flow condition on either side of the inlet port has been determined to be a result of the manifold aerodynamics rather than obstructed channels because it is reproducible in both SN 1 and SN 2 chambers. The locally low flow conditions, although acceptable for the technology program, will tend to result in undesirable thermal gradients around the chamber periphery and thus be detrimental to chamber life. When the chamber was flowed with double inlet ports, 180 degrees apart, flow distribution was improved. A somewhat more elaborate manifold or baffling will be recommended for future single inlet designs to improve this condition.

Similar cold flow test data for the SN 1 60-channel regeneratively cooled chamber are shown in Figure 4. The coolant inlet manifold in this design is fed at two locations spaced 180 degrees. All channels were found to be open and flowing uniformly within a range of $\pm$10%. This flow condition is considered satisfactory.

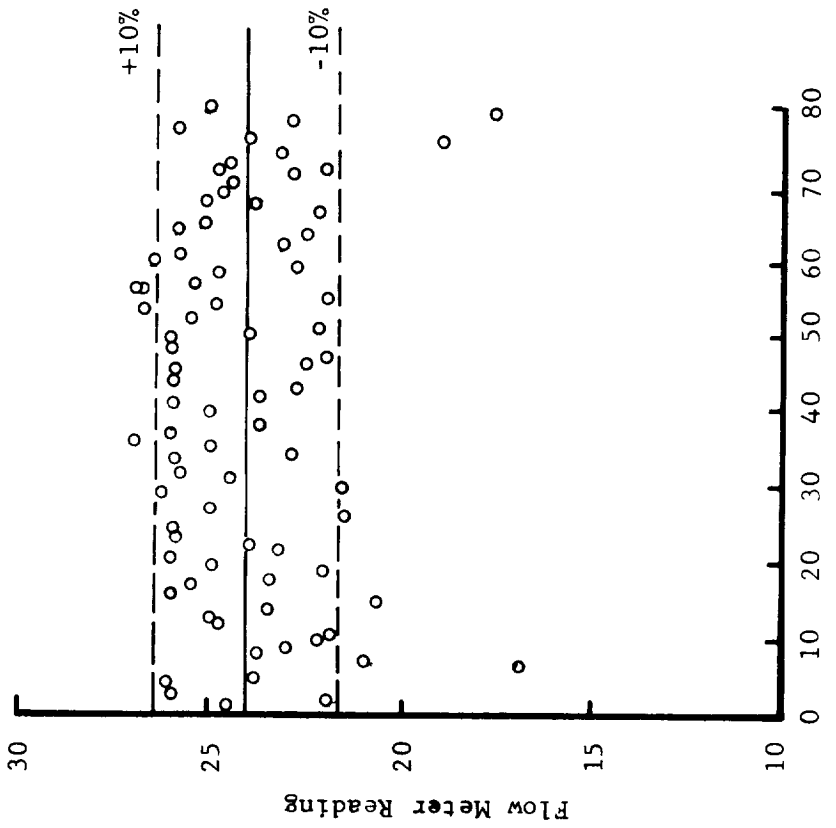

Figure 3. SN 2 Film-Cooled Chamber Coolant Jacket Flow Distribution

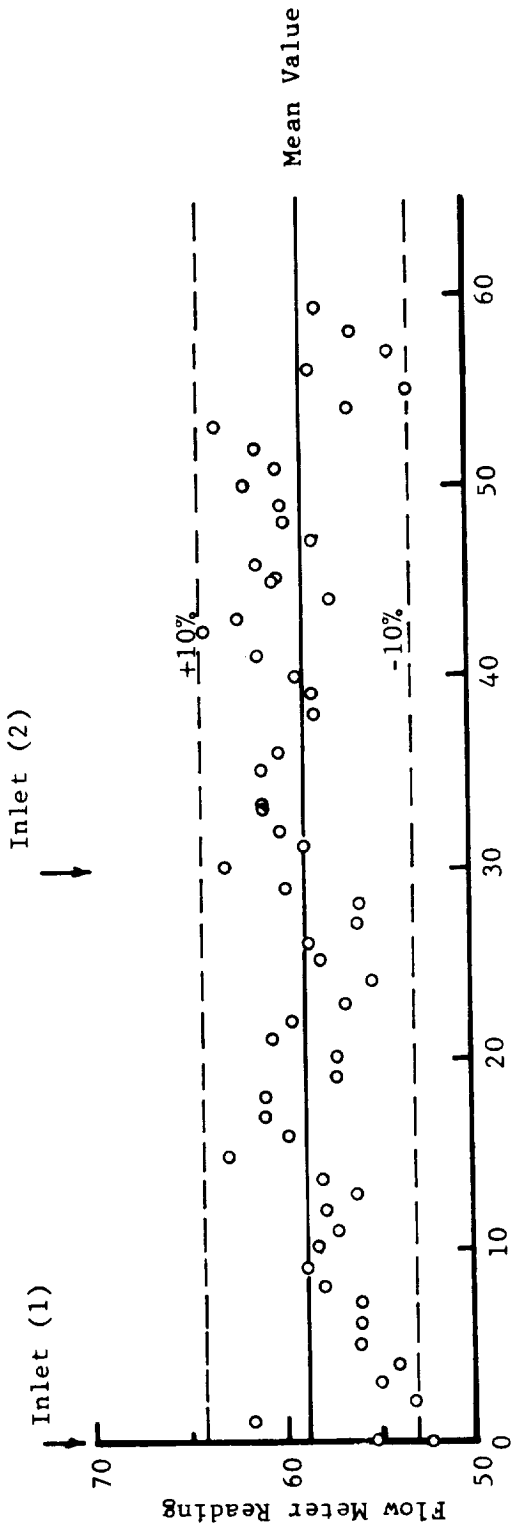

Figure 4. SN 1 Regeneratively Cooled Chamber Coolant Channel Flow Distribution

III, A, Activities for Ambient Temperature Propellants (cont.)

3. Task V - Igniter Design and Analysis - No activity.

4. Task VI - Igniter Checkout Tests - No activity.

5. Task VII - Valve Preparation - No activity.

6. Task VIII - Injector Checkout Tests

No new activities were conducted on this task; however, some of the test results are still being reviewed. Section III,A,3 in Report 14354-Q-3 presented the thermal characteristics of heat sink copper chambers with and without the use of film cooling. Two significant factors were noted. One was the experimental verification of the thermal model which predicted higher heat transfer coefficients when fuel film cooling is employed. The other was an observation that the heat flux vs wall temperature curves contained a higher-than-predicted value at low wall temperatures (early time in the run). Further analysis of the engine start transient dynamics in the Bay 7 test facility which employed critical flow nozzles fed through a pressure regulator is shown in Figure 5. This plot shows the engine and facility flow parameters vs time in the upper half and throat heat flux vs time in the lower half. The prefire pressures at which the regulators are set are higher than steady state to accommodate regulator-to-venturi line losses. This results in a correspondingly higher propellant weight flow during the first few tenths of a second after the thrust chamber valves are opened. These initially higher weight flows, in turn, result in the momentarily higher heat flux. When the data (solid points) in Figure 5 are adjusted to the steady-state flow rate, a lower heat flux (half shaded points) results. The adjusted heat flux is 15 to 20% lower in the early times and would reduce the heat transfer coefficients calculated from short tests in the copper chamber by a like amount. This correction makes the short duration copper chamber data of Figure III-7, Report 14354-Q-3, agree reasonably well with both the longer tests on the thin wall steel chamber and the heat transfer model predictions.

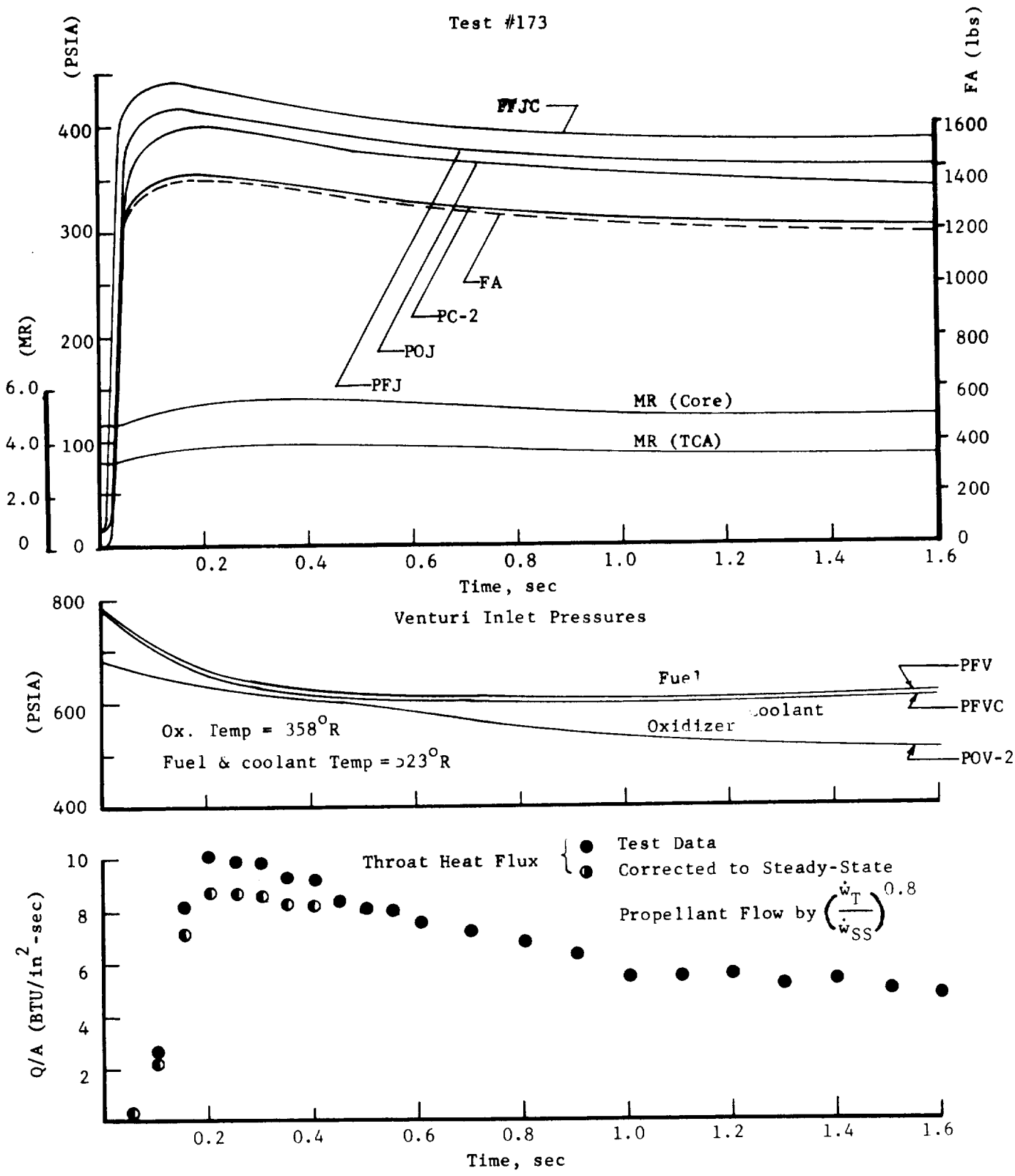

Figure 5. Physics Lab Bay 7 Thrust Chamber Start Transients Using Critical Flow Control Venturis

Test Parameter Nomenclature

F	Thrust
PFJ	Injector Fuel Manifold Pressure
POJ	Injector Oxidizer Manifold Pressure
PC	Chamber Pressure
PFV	Venturi Inlet Pressure, Fuel
POV	Venturi Inlet Pressure, Oxidizer
PFVC	Venturi Inlet Pressure, Film Coolant
MR	Mixture Ratio

III, A, Activities for Ambient Temperature Propellants (cont.)

The above discussion does not apply to the performance data since performance is based on a summary period which starts at 1.0 sec.

7. Task IX - Cooled Chamber Testing

a. Test Facility

Testing of 40:1 nozzle thrust chamber assemblies in the J-3 altitude facilities was initiated during this report period. This facility provides the capability of holding ambient pressures of less than 0.5 psia for up to several thousand seconds and sustained fire durations of 500 sec. The facility also contains an on-line computer (analog) which both controls and monitors critical engine operating parameters. The control of propellant flow rates (and thus thrust and mixture ratio) is accomplished via three flow control valves, i.e., fuel, oxidizer, and fuel film cooling. The computer holds the preselected respective flow rates by positioning each flow control valve to maintain a specified pressure at the inlet to critical flow venturis using both venturi inlet pressure and temperature measurements in the feedback loop. The computer is preprogrammed to provide TCA mixture ratios of 3, 4 and 5, with either 20, 25 or 30% film cooling at each MR, and to balance for either 100, 300 or 500 psia chamber pressures. Other film cooling flow rates can be programmed in by simply setting a dial. Mixture ratios and cooling flow rates can be changed by signal from the control console while the engine is firing.

The computer further monitors up to six engine parameters (temperature or pressure) and provides a means of automatically shutting down if values are not within specified safe operating ranges. Parameters normally monitored are injector face, nozzle throat and skirt temperatures and chamber pressure. The chamber pressure shutdown criteria require pressure to be obtained 0.03 sec after the oxidizer valve starts to open. All valves are signaled to close if this is not attained. To date the only computer shutdowns experienced were due to faulty temperature signals to the computer.

III, A, Activities for Ambient Temperature Propellants (cont.)

b. Summary of Testing (Series 1680-D03-0A)

Testing in this task is summarized in Table I. In order to check out the dynamics of the computer controlled system during mixture ratio changes and obtain a performance base point for comparison of J-3 altitude vs Physics Lab Bay 7 (Task VIII) data, initial J-3 tests were conducted with residual Task VIII injectors and 3:1 area ratio film-cooled steel chambers.

Tests 001 through 004 were valve, igniter sequence, and cold flow tests.

Tests 005 through 009 were system debugging and calibration tests with SN 2 I premix injector, a 3:1 area ratio film-cooled chamber, and a 25-lb-thrust spark igniter. Tests were conducted at partial altitude conditions to prevent accumulation of combustible gases in the test cell.

Tests 005, 006 and 007 were terminated between 0.6 and 1.0 sec by computer because of programming errors in the temperature shutdown criteria. Data points were obtained at TCA mixture ratios of 4, 3, 3, with nominal 30% film cooling.

Tests 008 and 009 with the same hardware were of 23 and 28 sec duration in which both film cooling and mixture ratio were varied while the engine was firing. Test 008 and Test 009 proceeded as follows:

Test	Period, sec	MR	% Cool
008	0 - 6	3.0	33
	7 - 11	3.0	30
	12 - 16	3.0	25.5
	17 - 20	3.0	33
	21 - 23	4.0	37
009	0 - 14	3.0	30
	15 - 28	4.0	35

TABLE I

SUMMARY OF TASK IX TESTS

Test No.	Date	Injector SN	Chamber	Data Summary Period, sec	L'/L*	P_c PFJI	TCA MR	% FFC	TCA W_t lb/sec	F_{Meas} lb	P_{Alt}	MR Core	F_{Vac} (Unc.)	I_{sv} Unc./Corr.	C^*	% C^* Unc. P_c-1A	% I_s
1680-003-0A																	
-001	System and Igniter Checkout Tests																
-002	System and Igniter Checkout Tests																
-003	System and Igniter Checkout Tests																
-004	System and Igniter Checkout Tests																
-005	4/30/71	2 I	3:1 FC	.4-.6	5.5/15	256	3.99	32.7	3.196	977.6	11.28	6.08	1075.6	336.5	7468		
-006	4/30/71	2 I	3:1 FC	.4-.96	5.5/15	269.4	3.000	32.05	3.237	1025.6	10.97	4.51	1120.9	346.3	7759		
-007	4/30/71	2 I	3:1 FC	.4-.91	5.5/15	268.0	3.022	31.4	3.23	1033.8	10.94	4.49	1128.8	349.5	7735		
-008	4/30/71	2 I	3:1 FC	15.0-20.0	5.5/15	250*	3.00	30.2	3.29	980.8	10.64	4.39	1073.2	326.2	7084*		
-009	4/30/71	2 I	3:1 FC	5-10	5.5/15	258*	2.93	29.7	3.29	1047.7	10.53	4.24	1139.2	346.2	7169*		
-010	5/12/71				7.5/20	Sea Level - Igniter Only											
-011	5/12/71					Altitude - Igniter Only											
-012	5/12/71					P_{Alt} 1A Bad No Perf. Dam.											
-013	5/12/71	5 I	40:1 FC/Cu	6.0-9.6		284.9	3.87	31.8	3.52	1354.9	1.037	5.87	1473.4	418.6/429.2	7438	90.3	90.7
-014	5/14/71	5 I	FC/Cu	30-35		290.2	3.96	30.6	3.52	1289.5	1.075	5.90	1412.4*	401.5/423.5	7583	92.3	89.5
-015	5/14/71	5 I	FC/Cu	20-50		290.0	3.93	30.6	3.50	1369.4	1.116	5.86	1497.0*	427.5/431.6	7583	92.0	91.2
				60-90		295.0	3.88	24.9	3.51	1389.3	1.161	5.33	1389.4*	433.8/437.9	7727	93.8	92.5
				100-130		298.4	3.86	19.4	3.51	1400.6	1.190	4.92	1536.7*	437.4/441.5	7804	94.7	93.3
				143-165		303.1	2.93	29.5	3.52	1385.5	1.237	4.26	1526.8*	434.2/439	7921	94.5	93.3
				173-193		306.1	2.92	25.3	3.52	1384.1	1.239	4.01	1525.7*	434/444	8004	95.5	94.4
				200-225		307.7	2.95	20.3	3.51	1381.2	1.232	3.79	1522.0*	434.1/448	8066	96.3	95.2
				245-270		278.3	4.84	30.0	3.51	1262.8	1.175	7.207	1397.1*	397.7/414	7278	91.1	87.9
-016	5/21/71	4 Trip	FC/Cu	Computer shut down due to amplifier malfunction													
-017	5/21/71	4 Trip	FC/Cu	4.0-5.0		291.0	2.95	28.6	3.36	1390.3	.615	4.24	1460.6	434.1	7948	94.9	92.3
				4.5-5.0		291.4	2.95	28.6	3.37	1389.2	.695	4.24	1468.6	436.0	7951	94.9	92.7
-018				4.0-4.5		296.5	2.94	25.4	3.41	1404.7	.728	4.04	1487.6	436.6	7995	95.4	92.8
				4.0-5.5		297.5	2.95	25.3	3.41	1387.0	.901	4.05	1489.9	436.5	8007	95.6	92.8
-019				.5-1.5		276.0	4.00	23.7	3.33	1390.9	.190	5.43	1412.6	424.8	7626	92.9	89.8
				3-8		284.4	3.98	25.1	3.43	1420.6	.346	5.49	1460.2	425.8	7622	92.8	90.0
				9.2-11.5		289.2	3.94	19.1	3.43	1412.8	.560	5.02	1476.8	430.5	7746	94.2	91.0
-020				.6-1.0		279.2	4.02	24.5	3.37	1404.1	.180	5.52	1424.6	423.3	7624	92.9	89.4
				4.0-6.0		285.4	4.00	24.9	3.44	1426.7	.331	5.51	1464.6	425.4	7618	92.8	89.9
				10.0-14.0		289.4	3.95	19.1	3.44	1399.0	.655	5.03	1473.8	428.3	7733	94.1	90.5
				17.0-22.0		279.5	4.03	30.5	3.42	1304.4	.970	6.01	1415.1	413.7	7507	91.5	87.4
				30-50.0		268.4	4.86	29.6	3.43	1345.1	.566	7.35	1409.7	410.5	7182	90.2	87.3
-021				5-50		93.9	4.44	21.4	1.15	464.3	.140	5.86	480.3	418.1	7514	92.7	88.5
				55-105		93.1	4.39	26.6	1.15	398.0	.140	6.22	474.4	411.8	7429	91.5	87.1
-022	6/15/71	4 Trip	FC/Cu	8-13	7.5/20	293.2	3.93	28.2	3.67	1377.4	1.535	5.5	1552.8	423.8	7338	90.8	91.3
-023	6/15/71			9-14		287.4	4.05	28.0	3.68	1364.0	1.289	5.7	1507.9	410.3	7187	89.2	88.5
				19-23		256.4	5.18	29.5	3.51	1221.5	1.243	7.4	1363.6	388.8	6719	86.1	84.2
				30-34		284.3	4.05	24.1	3.63	1389.1	1.126	5.4	1517.7	413.3	7134	88.8	88.6
				36-50		282.7	4.13	20.0	3.63	1346.1	1.451	5.2	1511.8	416.6	7158	89.0	89.9
				54-58		285.7	4.08	23.9	3.63	1308.4	1.692	5.4	1308.5	413.6	7230	89.7	89.2
-024	6/18/71			5-16		479.5	3.95	29.0	5.80	2416.3	.783	5.6	2505.8	432.0	7596	93.2	91.2
				19-23		486.1	3.92	24.3	5.81	2459.9	.728	5.2	2543.2	438.1	7694	93.4	92.5
				26-34		480.3	3.95	29.0	5.80	2439.4	.731	5.6	2522.9	434.9	7607	92.4	91.8

III, A, Activities for Ambient Temperature Propellants (cont.)

Accumulation of moisture in the load cell due to operation at partial vacuum resulted in questionable thrust measurements in the latter tests of this series. The facility, however, appeared to be operational at this point.

Tests 010 through 015 were conducted with SN 5A premix I-triplet injector, SN 1 film-cooled 40:1 nozzle, and the same spark igniter. Test 010 consisted of three igniter-only firings prior to evacuating the cell. Normal ignition was achieved in each case. Test 011 was a repeat series at altitude of 69,000 ft. The igniter was fired three times in series and three normal igniter ignitions were achieved. Test 012 was a 1-sec thrust chamber firing, MR = 4.0, 30% film cooling. Real time data playback indicated that all thermal and pressure parameters appear to function as predicted. The same test conditions were immediately repeated without hardware inspection in Run 013 for a 10-sec duration. Postfire inspection following the 10-sec test revealed the hardware to be in excellent condition.

The above test conditions were repeated for a 37-sec run (Test 014) during which steady-state temperatures were achieved throughout the nozzle.

Test 015 was initiated immediately following a brief data review and lasted for 278 sec. During this continuous fire period, the 11 following nominal balance conditions were evaluated:

MR	Data Points	% Film Cooling
4	(a - d)	30, 25, 20, 30
3	(e - h)	30, 25, 20, 30
4	i	30
5	j, k	30, 25

III, A, Activities for Ambient Temperature Propellants (cont.)

Testing was terminated due to a significant rise in cell pressure caused by depleted levels in the facility steam accumulator/ejector system. Steady-state thermal conditions were achieved at each condition except the last. Postfire hardware inspection revealed major local damage to the injector face under the oxidizer inlet, no damage to the chamber, igniter, facility, or instrumentation. Data analysis revealed failure was initiated 18.5 sec prior to shutdown and was undetected because of only minor changes in the temperature, pressure, and performance parameters being monitored. The failure is believed to have resulted from foreign material which came from the oxygen heat exchanger and lodged in the injector during the high oxygen flow (MR = 5) testing. Figure 6 shows a photograph of the film-cooled thrust chamber assembly mounted on the test stand within the J-3 altitude test cell prior to testing. Figure 7 shows the same nozzle after Test 015 at which time four restarts and 326 sec of duration had been accumulated. Figures 8 through 11 provide a graphical record of the propellant flow rates and some of the pressure and temperature parameters monitored during Test 015. Instrumentation location and nomenclature is identified in the third quarterly report. Changes in flows, and thus chamber wall temperatures, throughout the run are initiated by the preprogrammed computer control system.

Runs 016 through 021 employed the same hardware except the SN 5A injector was replaced by SN 4 premix triplet, which was employed earlier in a 2500-pulse test series in Bay 7 of the Physics Lab. Run 016, a repeat test at MR = 3.0, 20% film cooling, was computer terminated due to an amplifier malfunction in one of the throat temperature circuits.

Runs 017, 018 and 019 were short (5 sec) tests to obtain repeat performance with SN 4 injector at the following conditions:

Run	MR	% Cooling
017	3	30
018	3	25
019	4	25
	4	20

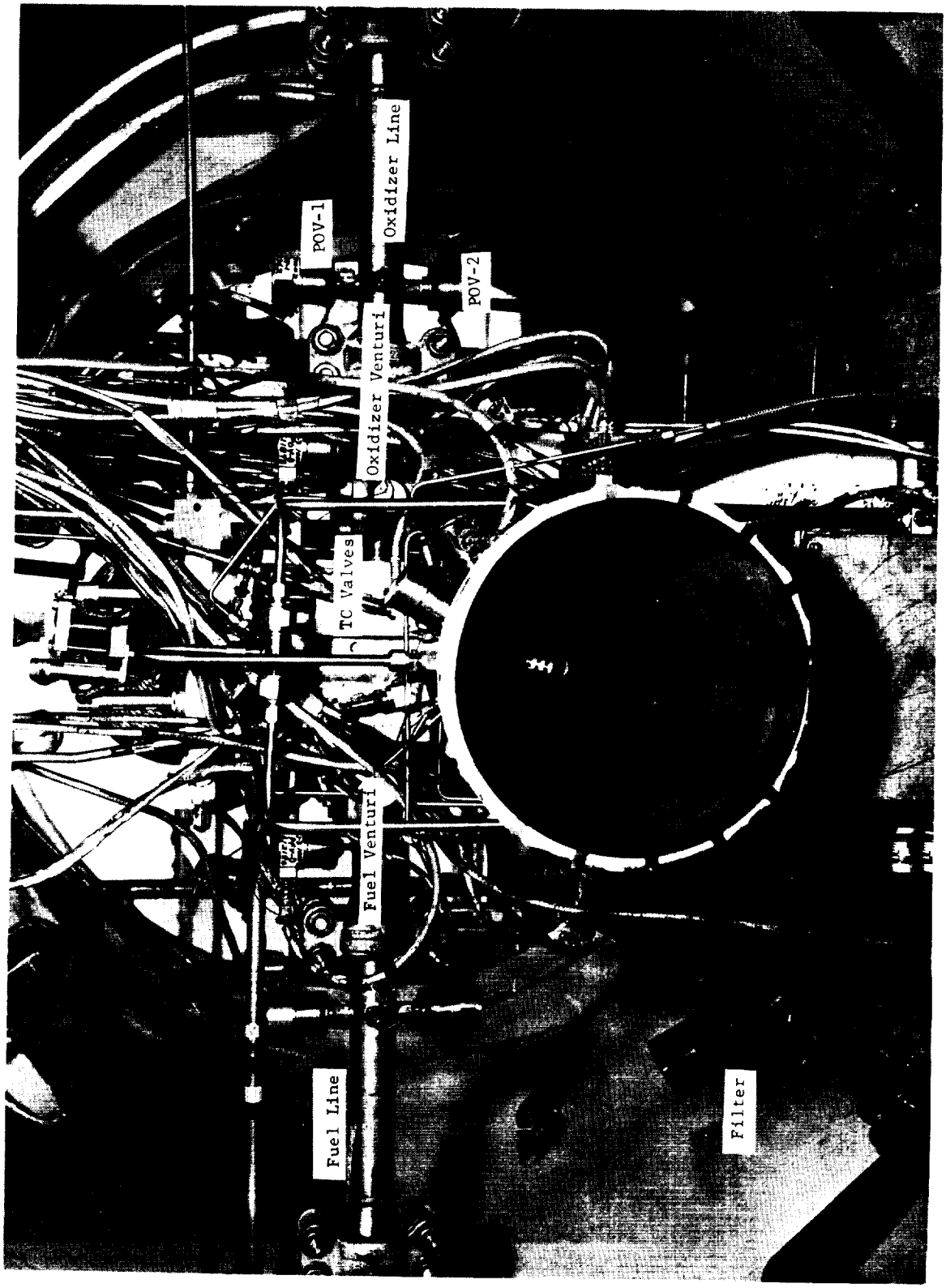

Figure 6. Film-Cooled Thrust Chamber Assembly on J-3 Altitude Facility (Prefire)

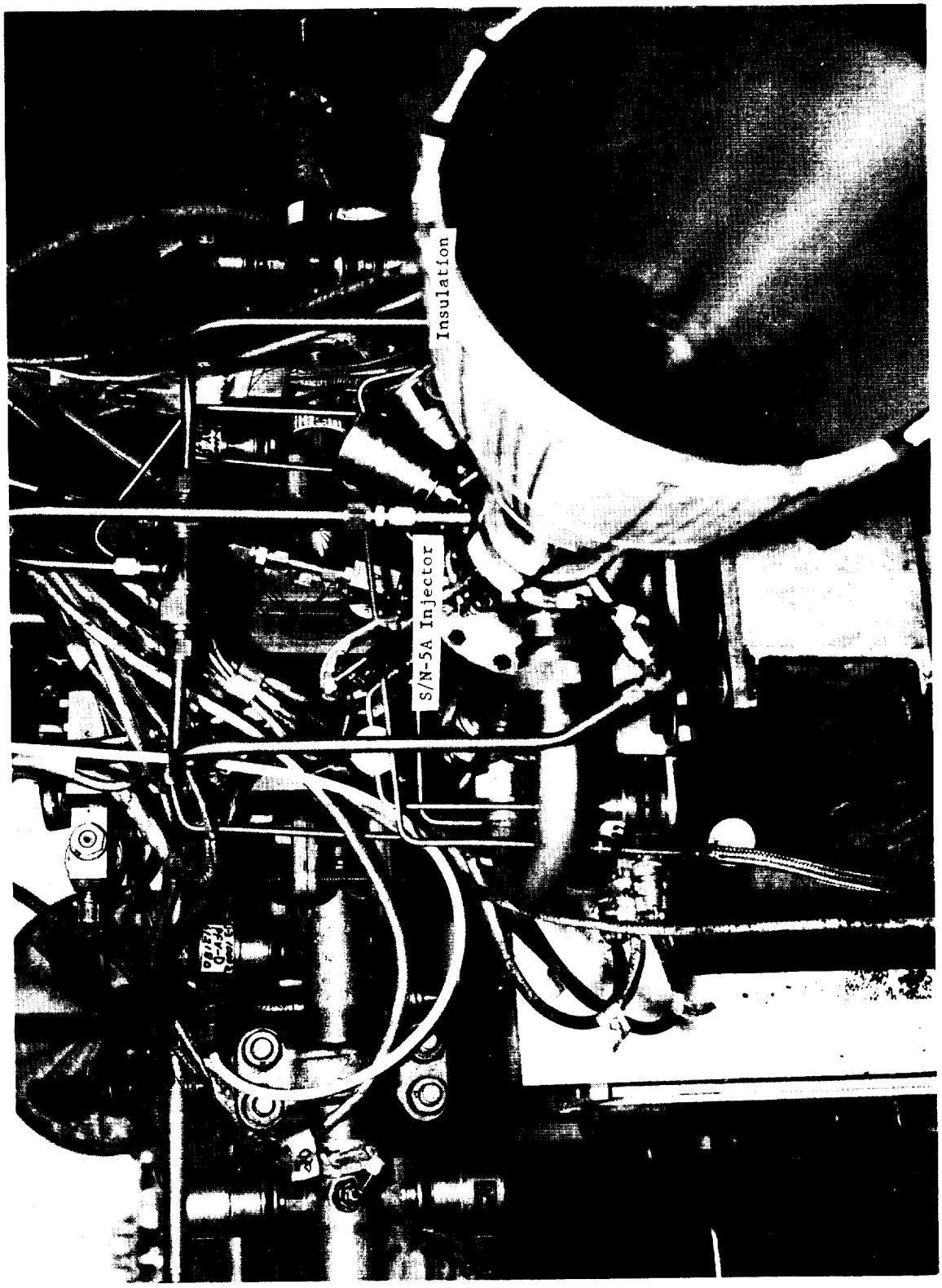

Figure 7. Film-Cooled TCA in J-3 Altitude Facility (Postfire)

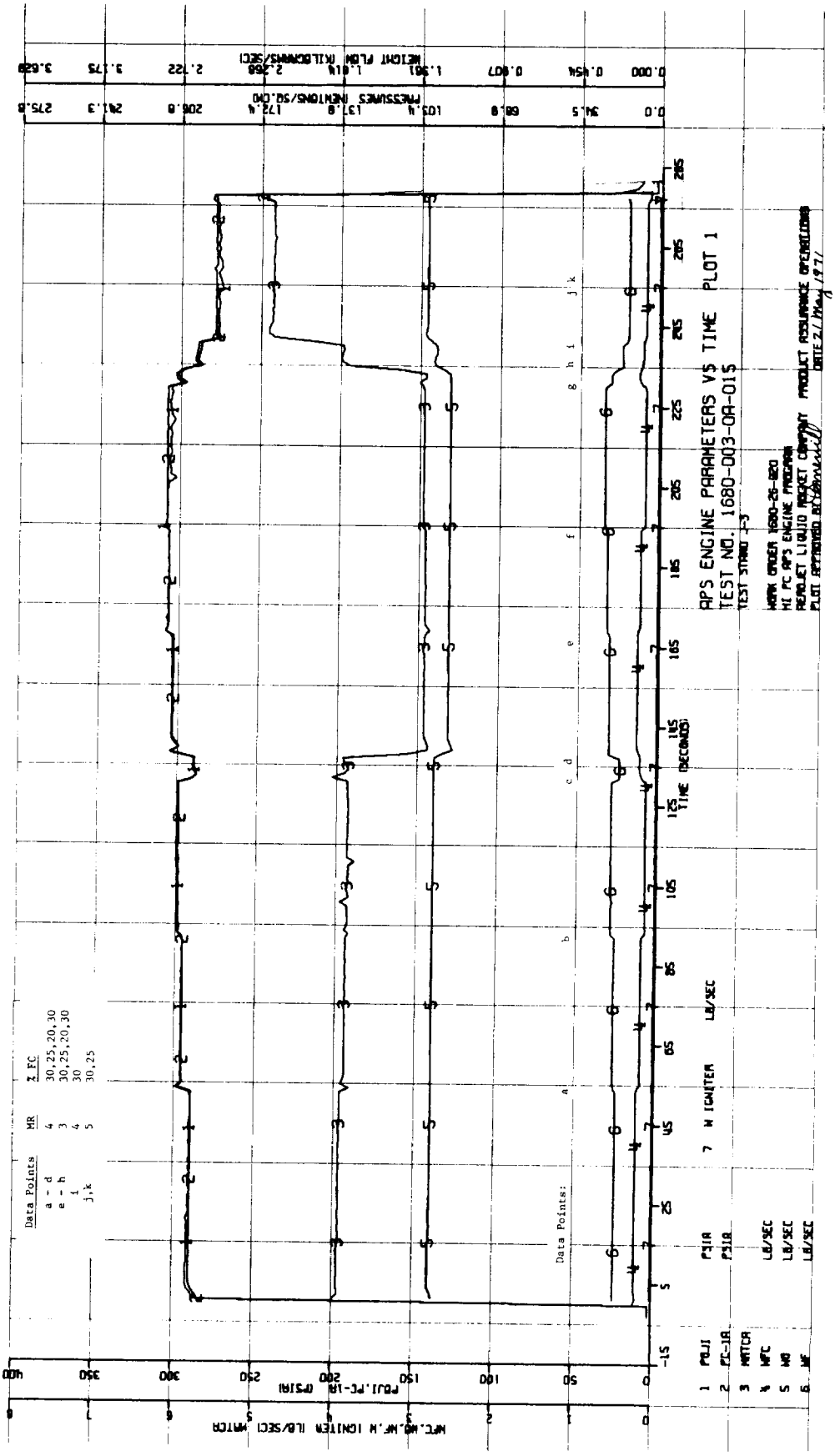

Figure 8. Computer Controlled Propellant Flow Rates

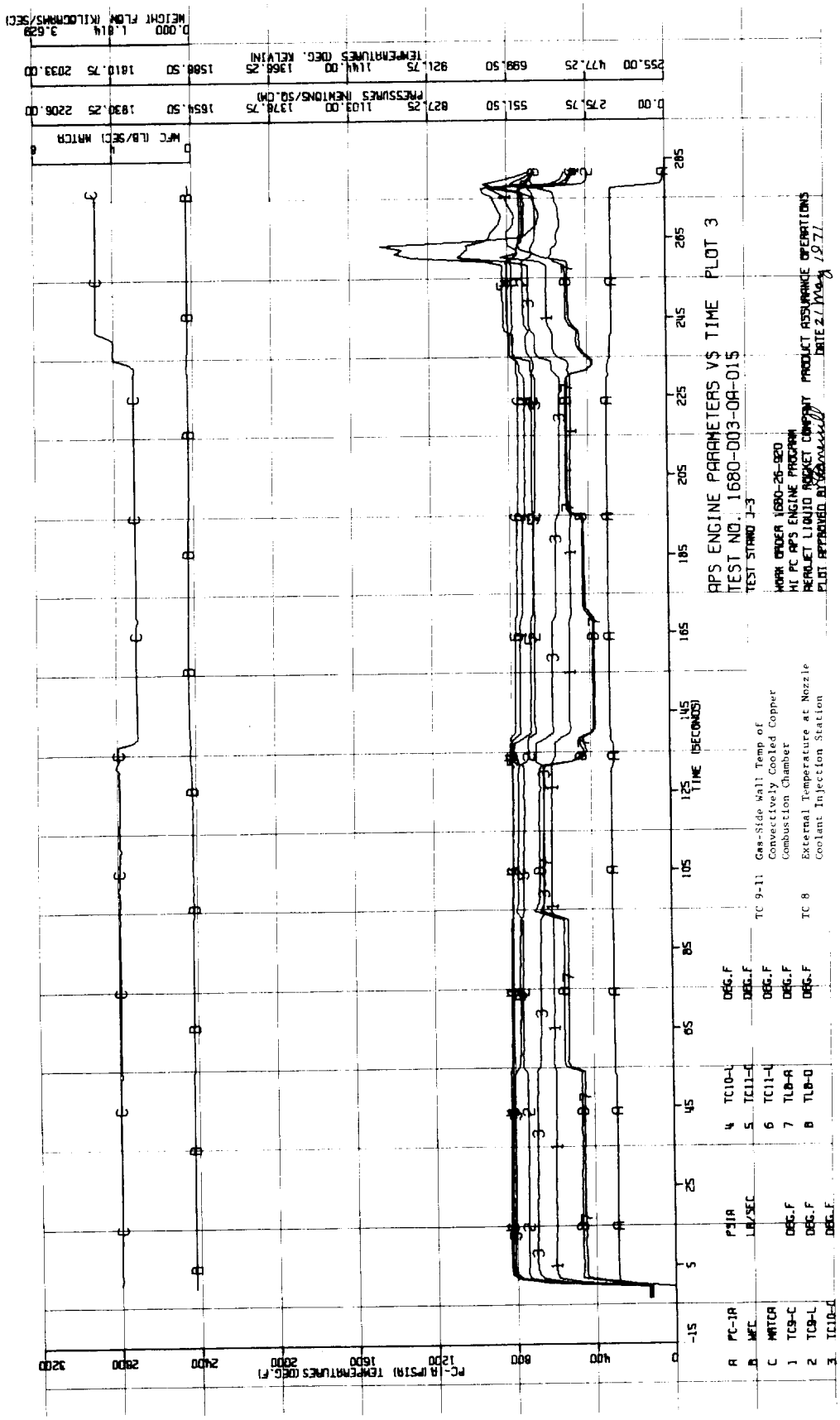

Figure 9. Thruster Wall Temperatures - Chamber Region

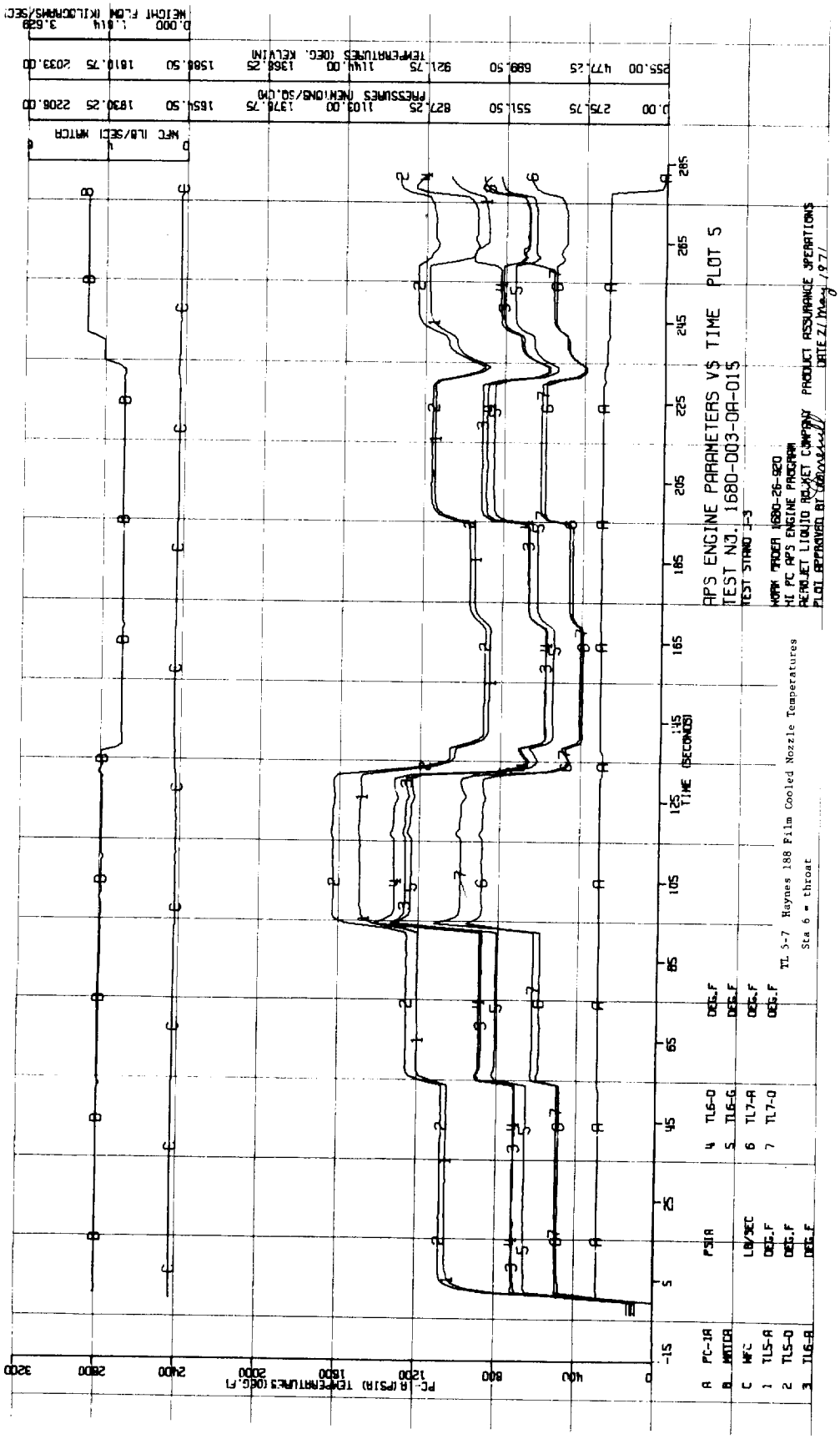

Figure 10. Thruster Wall Temperatures - Throat Region
(TL-7 Upstream, TL-6 Throat, TL-5 Downstream)

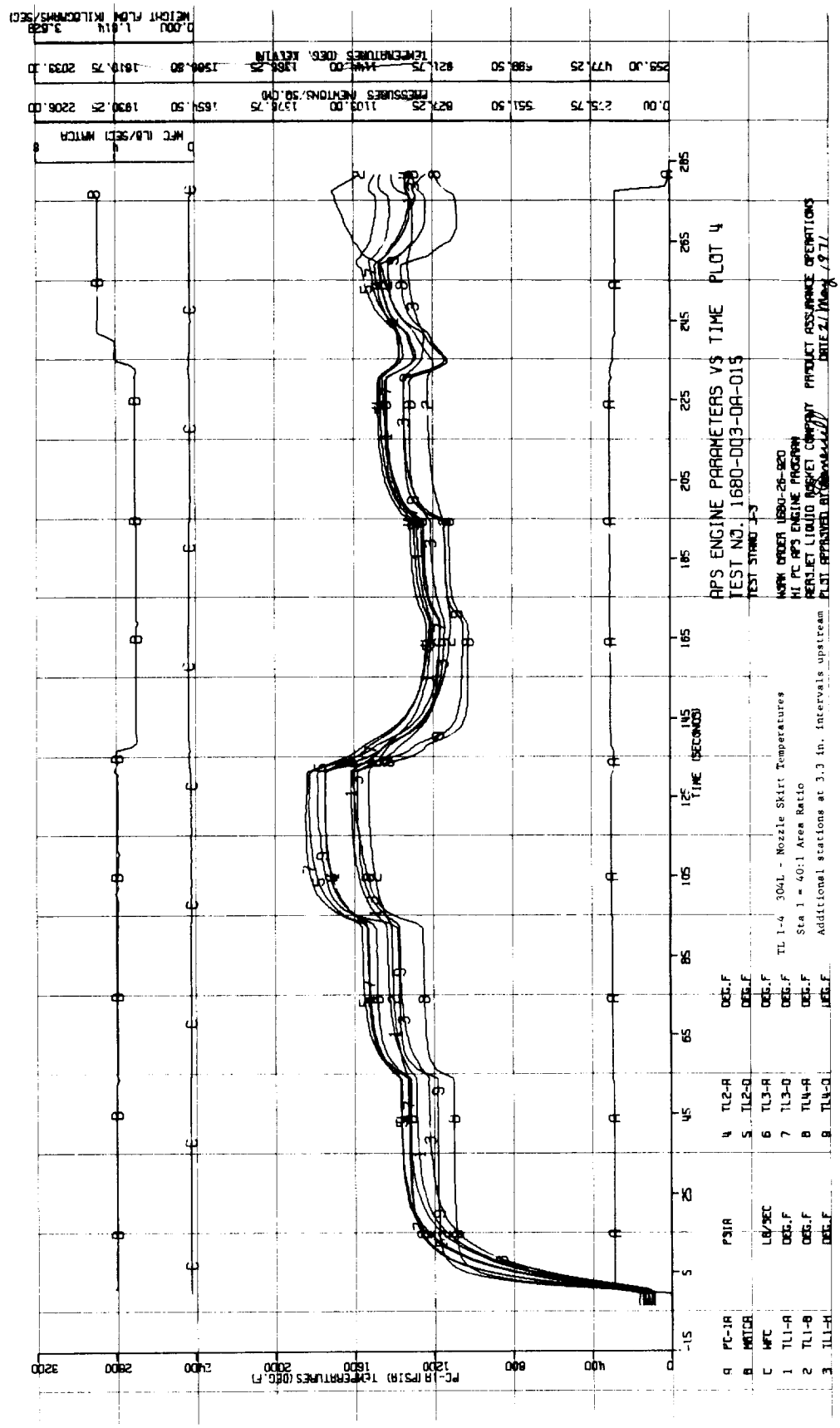

Figure 11. Thruster Wall Temperatures - Skirt Region

III, A, Activities for Ambient Temperature Propellants (cont.)

Run 020 was approximately 50 sec duration during which near steady wall temperatures were reached at the following conditions:

MR	% Cooling
4	25,20,30
5	30

Limiting wall temperatures were approached at the last test condition.

Run 021 was at reduced chamber pressure (100 psia) for a duration of 109 sec. Steady-state thermal conditions were achieved at a mixture ratio of 4.0 with 21 and 26% film cooling.

Tests 022 and 023 were low temperature propellant tests with the same hardware. A considerable amount of heat exchanger cold flow testing and evaluation of procedures for facility chilldown were conducted prior to this first cold propellant test series. The method of controlling propellant temperature is to adjust the LN_2 levels in the pool boiling heat exchangers. Cold flow tests showed that 200°R hydrogen could be delivered to the thrust chamber valve at fire switch and thereafter when the accumulator and feed lines were preconditioned with a LN_2 purge and the heat exchanger operated at maximum cooling capacity. The oxidizer heat exchanger has a much larger cooling capacity and care must be taken not to condense the GO_2 in the LN_2 bath. The initial oxygen circuit cold flow test was conducted with 50% of the pool boiling surface immersed in LN_2. Two phase flow was experienced in this run. Levels corresponding to 25 and 10% surface coverage were then flowed at nominal GO_2 flow rates. The latter coolant level provided the lower temperature limit of 320°R at the inlet of the critical flow venturi. Temperatures at the oxidizer valve were 12°F lower due to the pressure loss in the flow nozzle. Test 022 was a 15-sec burn at mixture ratio = 4 with 30% film cooling flow. The fuel temperature was 200°R and the oxidizer nominally 360°R

III, A, Activities for Ambient Temperature Propellants (cont.)

throughout the run. Performance data on this test was of questionable value because of high cell pressures resulting from the GN_2 cell purges which were left on during the test.

Test 023 was a repeat test of 58-sec duration. The nominal test objectives were MR = 4.0, 30 and 25% cooling. A wider range of test conditions were actually demonstrated due to an invalid temperature signal to the computer. Nominal flow conditions experienced in this test were as follows:

Period, sec	MR	% Cooling	T_{fuel}, °R	T_{ox}, °R
0-15	4	28	200	320
15-25	5	28	200	320
30-45	4	20	200	320

Test 024 was a high pressure (500 psia) ambient temperature propellant run of 34 sec duration. Nominal test conditions were:

MR	% Cooling
4	30,25,30

Limiting skirt temperatures of 1850°F were approached at the 25% coolant flow conditions.

Hardware inspections following each of the three preceding tests showed all components to be in excellent condition. Figure 12 shows the SN 4 triplet injector following these tests; at this time, the injector had accumulated over 700 sec duration and 2600 restarts.

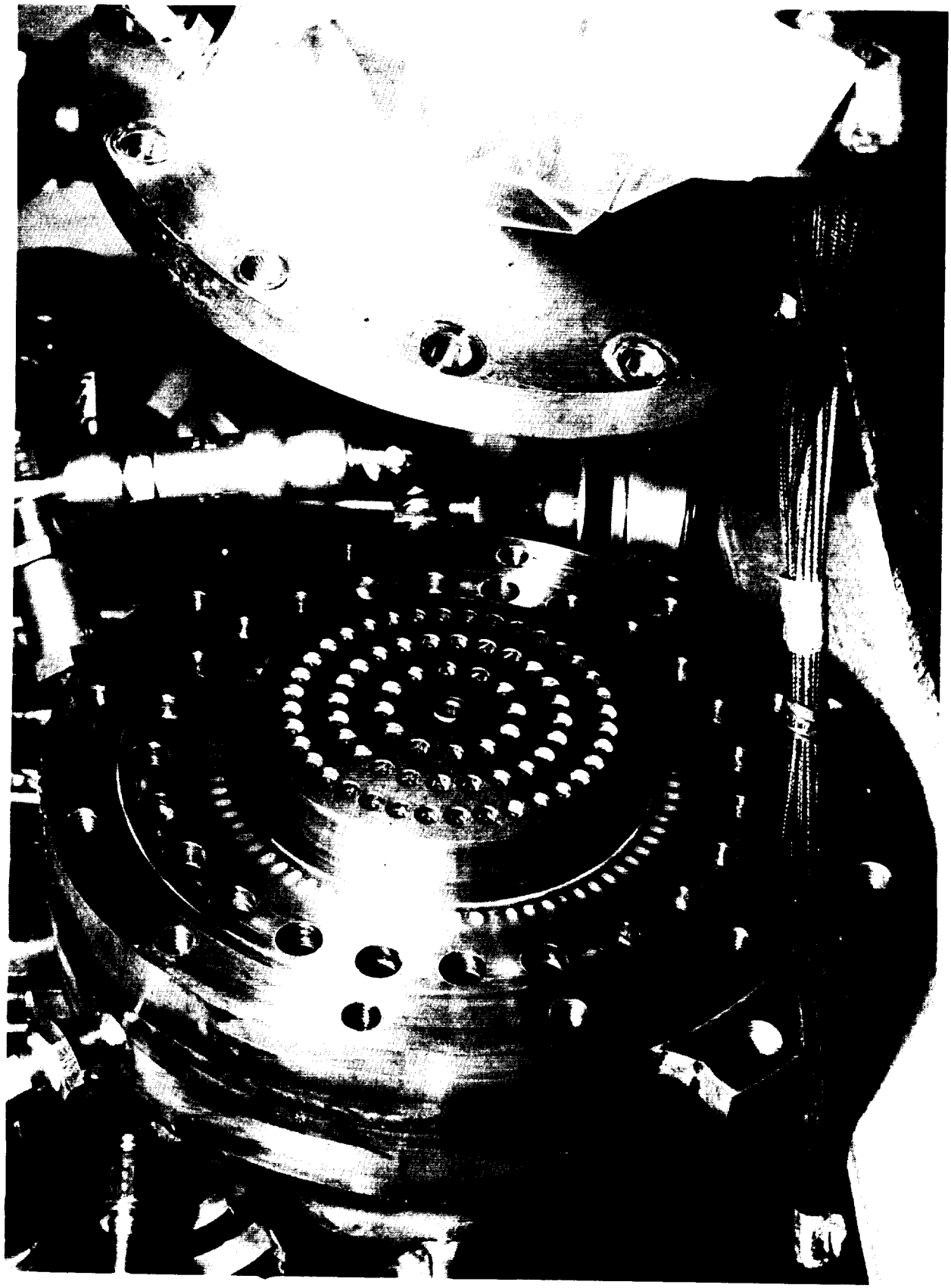

Figure 12. SN 4 Triplet Injector After 2600 Restarts and 700 sec Firing

III, A, Activities for Ambient Temperature Propellants (cont.)

In the process of temperature conditioning the feed system prior to Run 025, which was to be a 500 psia cold propellant test, a small H_2 pop outside of the altitude cell ruptured a facility hydraulic line and caused a small oil fire outside the cell. This resulted in some damage to facility equipment located nearby. There was no damage within the test cell since it was sealed and at high vacuum conditions.

c. Test results

Summary

Test conditions, duration and performance are summarized in Table I. The performance results should be considered preliminary because of an accumulation of small discrepancies in thrust measurements. In some tests, two performance values are provided. The first is the Vac I_{sp} computed from the uncorrected thrust measurements. The second is calculated from the corrected thrust measurements. The performance data (Vac I_{sp} and uncorrected c*) provided in Table I are presented graphically in Figure 13, while a summary of the axial temperature profiles at the various test conditions and critical temperatures vs film cooling flow are presented in Figures 14, 15, 16 and 17.

This initial test series has essentially demonstrated the feasibility of the film-cooled chamber design and its ability to operate over a wide range of mixture ratios. Film cooling flow rates as low as 19% at nominal design conditions were attained while still maintaining throat and nozzle temperatures which are compatible with long life. Maximum throat and skirt temperatures at the minimum film cooling flow rates were 1250 and 1850°F, respectively. The capability of meeting or exceeding the performance goal of 435 sec specific impulse with the premix I-triplet injector configuration is indicated by the performance data. These data also indicate a 7- to 10-sec performance differential between the I-triplet and triplet injector patterns.

TABLE I

SUMMARY OF TASK IX TESTS

Test No.	Date	Injector SN	Chamber	Data Summary Period, sec	L'/L*	P_c FFJI	TCA MR	% FFC	TCA W_t lb/sec	F_{Meas} lb	P_{Alt}	MR Core	Prop. Temp.	F_{Vac} (Unc.)	I_{sv} Unc./Corr.	C*	% C* Unc. P_c-1A	% I_s
1680-D03-0A																		
-001	System and Igniter Checkout Tests																	
-002	System and Igniter Checkout Tests																	
-003	System and Igniter Checkout Tests																	
-004	System and Igniter Checkout Tests																	
-005	4/30/71	2 I	3:1 FC	.4-.6	5.5/15	256	3.99	32.7	3.196	977.6	11.28	6.08	Amb.	1075.6	336.5	7468		
-006	4/30/71	2 I	3:1 FC	.4-.96	5.5/15	269.4	3.000	32.05	3.237	1025.6	10.97	4.51		1120.9	346.3	7759		
-007	4/30/71	2 I	3:1 FC	.4-.91	5.5/15	268.0	3.022	31.4	3.23	1033.8	10.94	4.49		1128.8	349.5	7735		
-008	4/30/71	2 I	3:1 FC	15.0-20.0	5.5/15	250*	3.00	30.2	3.29	980.8	10.64	4.39		1073.2	326.2	7084*		
-009	4/30/71	2 I	3:1 FC	5-10	5.5/15	258*	2.93	29.7	3.29	1047.7	10.53	4.24		1139.2	346.2	7169*		
-010	5/12/71				7.5/20	Sea Level - Igniter Only												
-011	5/12/71					Altitude - Igniter Only												
-012	5/12/71					P_{Alt} 1A Bad No Perf. Dam.												
-013	5/12/71	5 I	40:1 FC/Cu	6.0-9.6		284.9	3.87	31.8	3.52	1354.9	1.037	5.87	Amb.	1473.4	418.6/429.2	7438	90.3	90.7
-014	5/14/71	5 I	FC/Cu	30-35		290.2	3.96	30.6	3.52	1289.5	1.075	5.90		1412.4*	401.5/423.5	7583	92.3	89.5
-015	5/14/71	5 I	FC/Cu	20-50		290.0	3.93	30.6	3.50	1369.4	1.116	5.86		1497.0*	427.5/431.6	7583	92.0	91.2
				60-90		295.0	3.88	24.9	3.51	1389.3	1.161	5.33		1389.4*	433.8/437.9	7727	93.8	92.5
				100-130		298.4	3.86	19.4	3.51	1400.6	1.190	4.92		1536.7*	437.4/441.5	7804	94.7	93.3
				143-165		303.1	2.93	29.5	3.52	1385.5	1.237	4.26		1526.8*	434.2/439	7921	94.5	93.3
				173-193		306.1	2.92	25.3	3.52	1384.1	1.239	4.01		1525.7*	434/444	8004	95.5	94.4
				200-225		307.7	2.95	20.3	3.51	1381.2	1.232	3.79		1522.0*	434.1/448	8066	96.3	95.2
				245-270		278.3	4.84	30.0	3.51	1262.8	1.175	7.207		1397.1*	397.7/414	7278	91.1	87.9
-016	5/21/71	4 Trip	FC/Cu	Computer shut down due to amplifier malfunction														
-017	5/21/71	4 Trip	FC/Cu	4.0-5.0		291.0	2.95	28.6	3.36	1390.3	.615	4.24	Amb.	1460.6	434.1	7948	94.9	92.3
				4.5-5.0		291.4	2.95	28.6	3.37	1389.2	.695	4.24		1468.6	436.0	7951	94.9	92.7
-018				4.0-4.5		296.5	2.94	25.4	3.41	1404.7	.728	4.04		1487.6	436.6	7995	95.4	92.8
				4.0-5.5		297.5	2.95	25.3	3.41	1387.0	.901	4.05		1489.9	436.5	8007	95.6	92.8
-019				.5-1.5		276.0	4.00	23.7	3.33	1390.9	.190	5.43		1412.6	424.8	7626	92.9	89.8
				3-8		284.4	3.98	25.1	3.43	1420.6	.346	5.49		1460.2	425.8	7622	92.8	90.0
				9.2-11.5		289.2	3.94	19.1	3.43	1412.8	.560	5.02		1476.8	430.5	7746	94.2	91.0
-020				.6-1.0		279.2	4.02	24.5	3.37	1404.1	.180	5.52		1424.6	423.3	7624	92.9	89.4
				4.0-6.0		285.4	4.00	24.9	3.44	1426.7	.331	5.51		1464.6	425.4	7618	92.8	89.9
				10.0-14.0		289.4	3.95	19.1	3.44	1399.0	.655	5.03		1473.8	428.3	7733	94.1	90.5
				17.0-22.0		279.5	4.03	30.5	3.42	1304.4	.970	6.01		1415.1	413.7	7507	91.5	87.4
				30-50.0		268.4	4.86	29.6	3.43	1345.1	.566	7.35		1409.7	410.5	7182	90.2	87.3
-021				5-50		93.9	4.44	21.4	1.15	464.3	.140	5.86		480.3	418.1	7514	92.7	88.5
				55-105		93.1	4.39	26.6	1.15	398.0	.140	6.22		474.4	411.8	7429	91.5	87.1

*Data questionable. Instrumentation calibration shift during test

TABLE I (cont.)

Test No.	Date	Injector SN	Chamber	Data Period	L'/L*, in/in	P_c, psia	TCA MR O/F	% FFC, % WFC/WFT	TCA WT, #/sec	F_{Meas}, lbs_f	P_{Alt}, psia	MR Core O/F	Prop. Temp. O_2/H_2, $^oR/^oR$	F_{Vac}, lbs_f	I_{sv}, sec	C*, ft/sec	$\%C^*$, %	$\%I_s$, %
1880-B03-0A																		
-022	6/15/71	4 Trip	FC/Cu	8-13	7.5/20	293.2	3.93	28.2	3.67	1377.4	1.535	5.5	355/208	1552.8	423.0	7338.1	90.8	91.3
-023	6/15/71			9-14		287.4	4.05	28.0	3.68	1364.0	1.289	5.7	321/199	1507.9	410.3	7187.3	89.2	88.5
				19-23		256.4	5.18	29.5	3.51	1221.5	1.243	7.4	319/202	1363.6	388.8	6719.8	86.1	84.2
				30-34		284.3	4.05	24.1	3.65	1389.1	1.126	5.4	324/235	1517.7	415.5	7154.5	88.8	89.6
				36-50		282.7	4.13	20.0	3.63	1346.1	1.451	5.2	331/232	1511.8	416.6	7158.7	89.0	89.9
				54-58		285.7	4.08	23.9	3.63	1308.4	1.692	5.4	339/238	1308.5	413.6	7230.2	89.7	89.2
-024	6/18/71			5-16		479.5	3.95	29.0	5.80	2416.3	.783	5.6	528/521	2505.8	432.0	7596.4	92.2	91.2
				19-23		486.1	3.92	24.3	5.81	2459.9	.728	5.2	528/521	2543.2	438.1	7694.3	93.4	92.5
				26-34		480.3	3.95	29.0	5.80	2439.4	.731	5.6	528/521	2522.9	434.9	7607.8	92.4	91.8

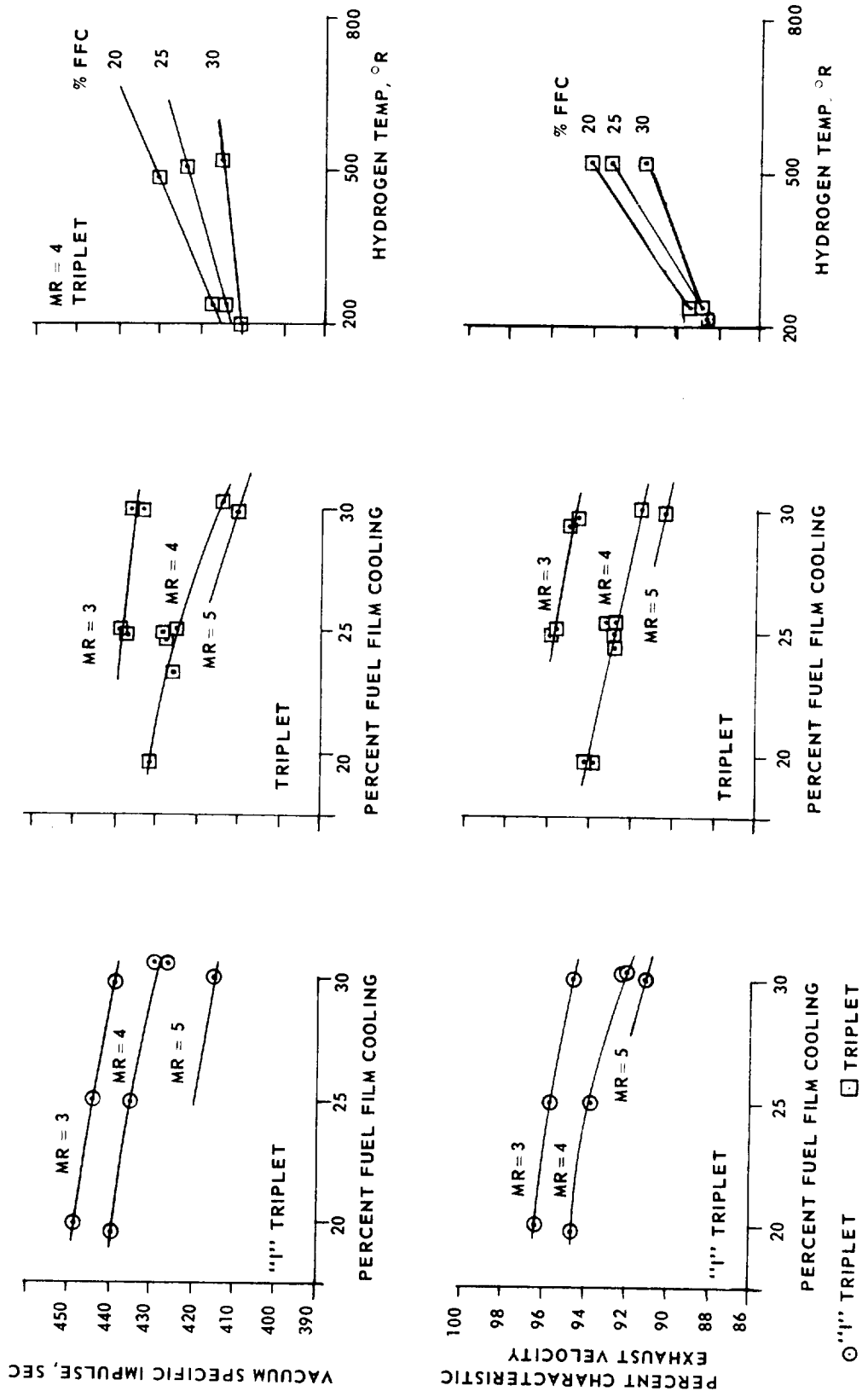

Figure 13. Film-Cooled Chamber Altitude Performance (ε = 40:1)

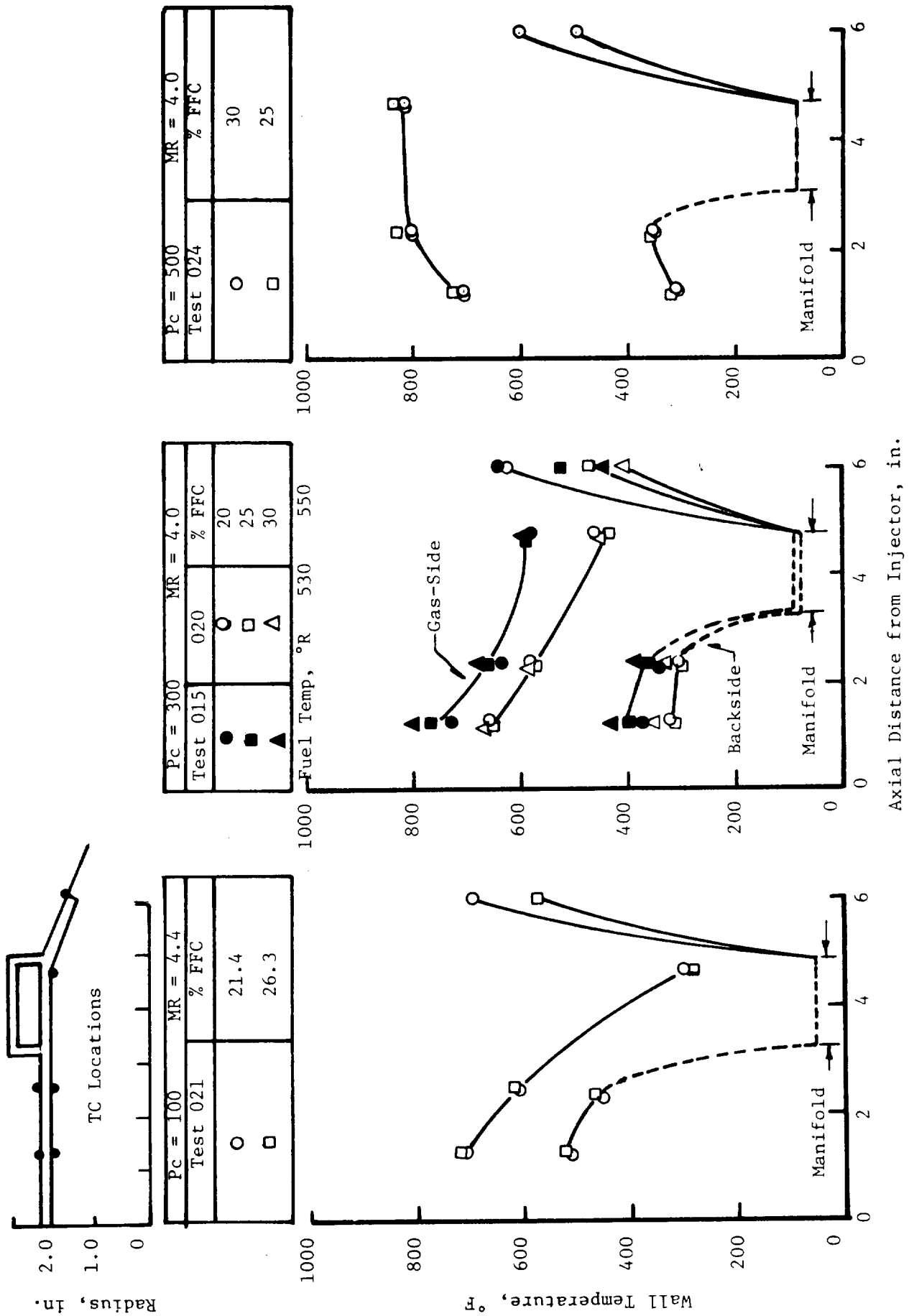

Figure 14. Film-Cooled Chamber Temperature Data (Chamber Region)

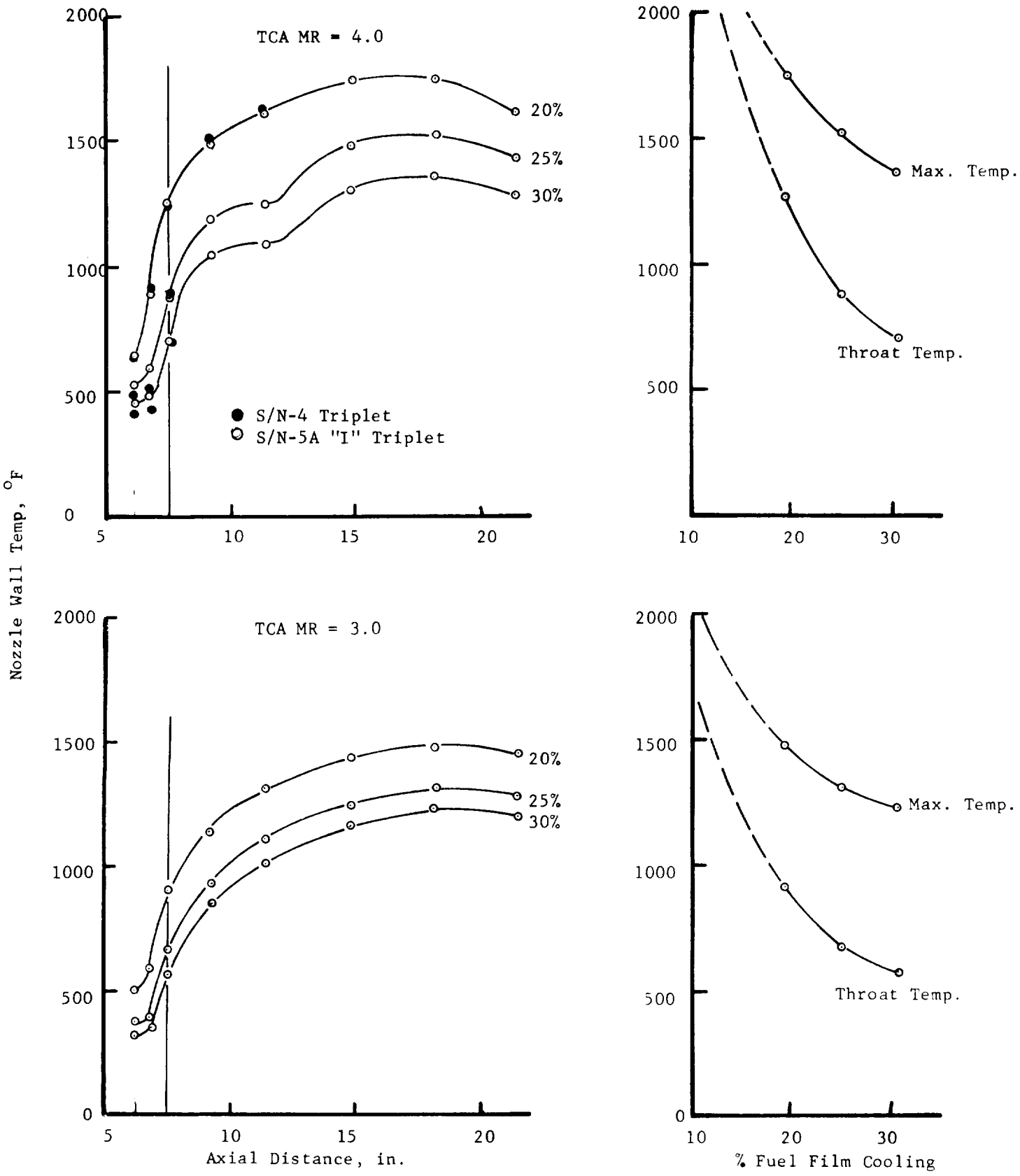

Figure 15. Film-Cooled Chamber Temperature Profiles, 300 psia (Throat and Skirt Region)

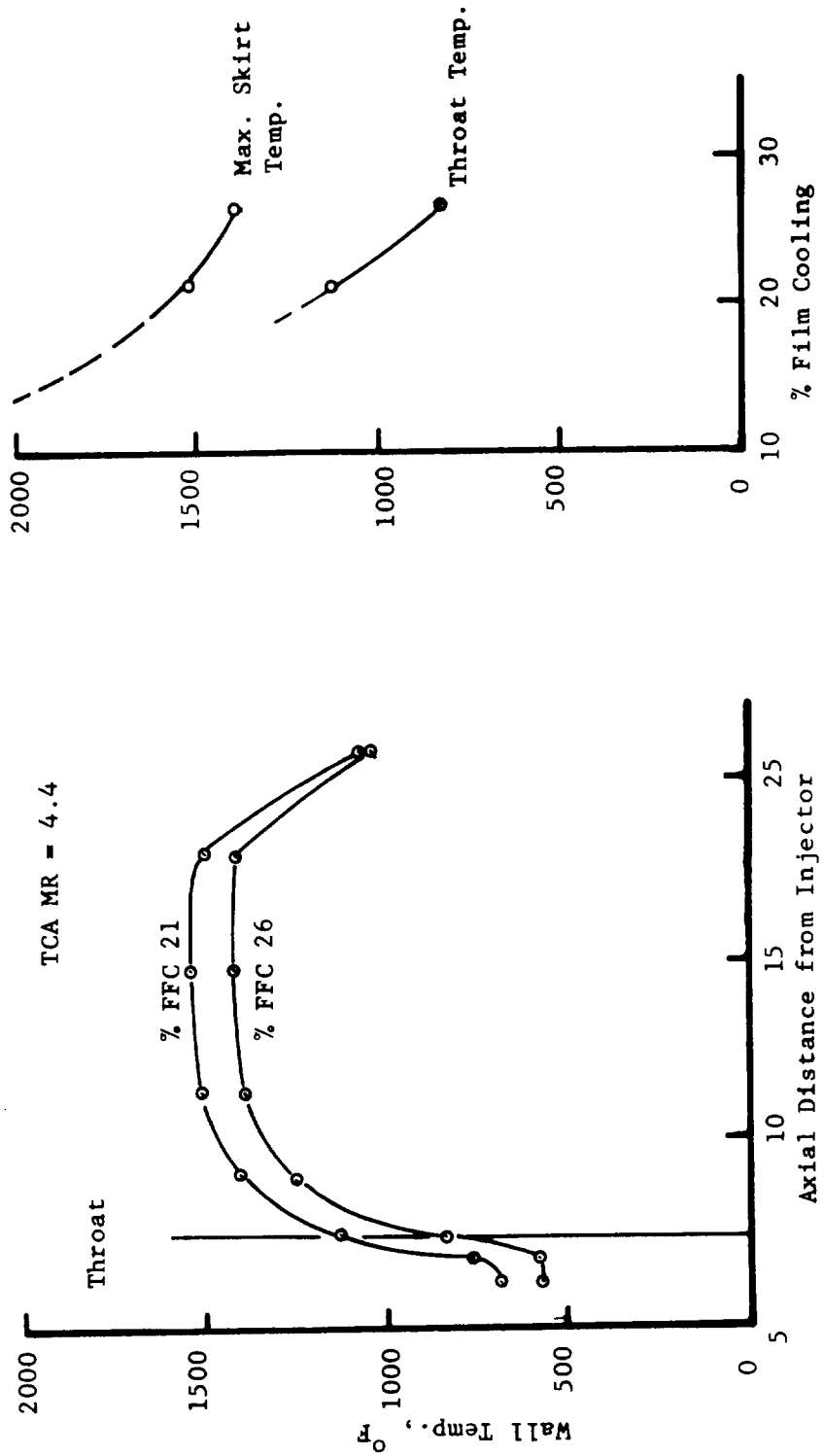

Figure 16. Film-Cooled Chamber Nozzle Temperature Profiles, 100 psia (Test 021)

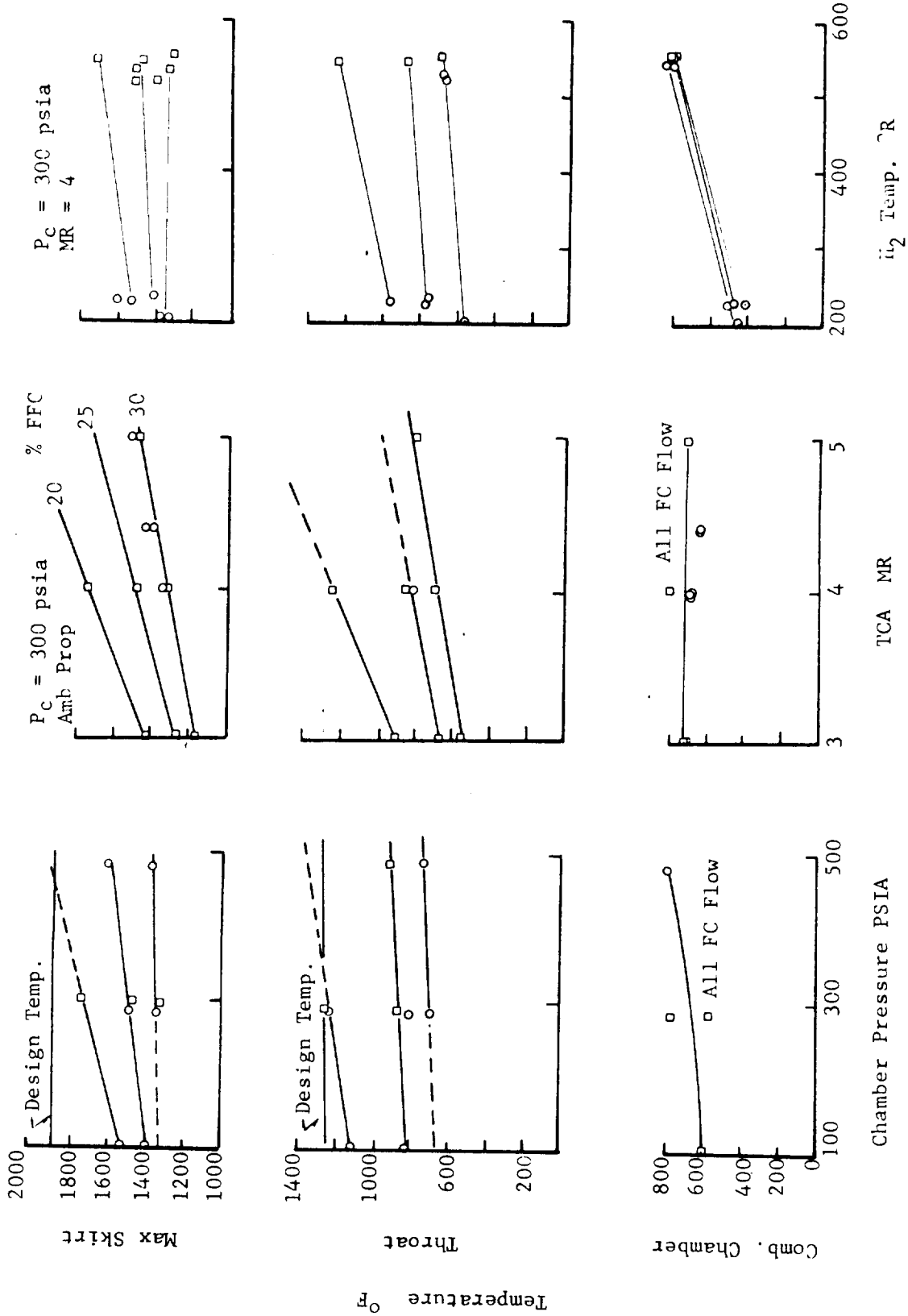

Figure 17. Film-Cooled Thrust Chamber Sensitivity

III, A, Activities for Ambient Temperature Propellants (cont.)

Both injectors produce the same axial temperature profile with the exception of the first three stations downstream of the face, at which point the "I" configuration showed about a 100°F higher wall temperature, indicative of more rapid combustion and substantiating the higher performance.

Thruster Performance

Performance data from the initial 24 altitude tests have been reviewed and are presented in Table I. All performance data are based on directly measured values with the exception of Tests 013 through 015*.

The resulting performance data are portrayed in Figure 13, denoting the influence of operating variables and injector type on measured vacuum specific impulse and percent characteristic exhaust velocity. Performance differences between the I-triplet and triplet injectors are shown on the left portion of the figure over a range of mixture ratios and coolant percentages. The I-triplet injector delivers "goal" performance (I_{sp} = 435 sec) at 27.5% coolant compared to 15% with the triplet injector. At 27.5% coolant fraction and mixture ratio 4.0, the I-triplet is operating at approximately 98% energy release efficiency. The triplet is approximately 3% lower.

These comparative data appear to the right of the "I" pattern data in Figure 13. Reductions in the hydrogen propellant temperature to 200°R produce impulse reductions of 9 sec at 25% coolant. This agrees quite favorably with a theoretical shift of 10 sec for the inlet propellant sensible enthalpy decrease.

*On these tests, a preload was recorded on both the standard and measuring thrust cells prior to ignition. This preload was relieved on the stand and cell as thrust was applied to the thrust frame and returned to a value consistent with the measuring cell on shutdown. A subsequent investigation revealed this preload was a result of ambient pressure acting on one side of the hydraulic actuator when the other side was vented to the altitude cell vacuum. Adding this bias to the measured values allowed generation of the corrected data, also presented in Table I. Including these corrections, the quoted measurement accuracy is 0.70% - 2σ.

III, A, Activities for Ambient Temperature Propellants (cont.)

Thermal Characteristics

Figures 14, 15, 16 and 17 summarize a portion of the steady-state combustion chamber, throat, and skirt thermal profiles for the film-cooled chamber. Figure 14 provides the measured gas-side and backside wall temperatures for the copper-lined combustion chamber and film coolant injector. Data are presented for chamber pressures of 100, 300 and 500 psia and film cooling flow rates corresponding to 20 to 30% of the fuel. Maximum copper wall temperatures are observed to increased from about 700°F at 100 psia chamber pressure to approximately 800°F at 500 psia, thus demonstrating the insensitivity of the combustion chamber temperature to operating pressure. Reduction of the film cooling employed for throat and skirt cooling also has a minimal influence on the combustion chamber temperatures. Reducing film coolant flows to optimize performance results in a small reduction in the chamber temperatures and slight increase in the temperature of the film coolant injector. The reduction in chamber temperature is a result of the increasing the percent of total fuel which flows through the regeneratively cooled portion of the chamber and injector. Figure 13 also provides a comparison of the chamber temperature profiles for the two injector patterns at 300 psia (solid "I" vs open data points for the triplet). The heat flux with the "I" pattern is slightly higher.

Figures 15 and 16 provide the axial temperature profiles for the film-cooled monowall portion of the nozzle. Data are provided for mixture ratios 3 and 4 at chamber pressures of 100 and 300 psia for film cooling flow of 20 to 30%. Cross-plots of throat temperature and maximum skirt temperature (insulated) are also provided. These data indicate that the design temperatures of 1200°F in the throat and 1800°F maximum in the skirt can be achieved with approximately 20% film coolant.

III, A, Activities for Ambient Temperature Propellants (cont.)

The thermal sensitivity of the film-cooled chamber to variations in chamber pressure, mixture ratio, and H_2 inlet temperature are given in Figure 17. These plots summarize the data obtained in the testing to date and provide considerable insight into the operation of the film-cooled chamber. Steady-state temperature data from three different nozzle locations are presented. The three locations shown are the critical ones in establishing the chamber operation and life. The maximum skirt temperature is the hottest part of the chamber and thus most susceptible to a failure from simple overheating. The throat is the most highly stressed part of the film-cooled shell and establishes the cycle life capability of the spun film-cooled nozzle. The combustion chamber temperature is key in establishing the cycle life of the regeneratively cooled portion.

The effect which chamber pressure has upon the maximum skirt temperature depends upon the coolant flow rate. At the 30% film cooling flow rate, the maximum skirt temperature is essentially independent of P_c, while at the 20% flow the maximum temperature increases gradually with P_c. This increasing temperature with P_c is a little surprising in that, ordinarily, film-cooled devices are favored by higher pressures. One possible explanation for what is occurring here is that the skirt is not truly adiabatic but rather is partially cooled by radiation out the nozzle exit. This would explain both the insensitivity to P_c at low temperatures associated with the 30% cooling flow and the increasing sensitivity to P_c at the higher temperatures associated with the lower coolant flows. What is significant is that the peak temperature condition (20% cooling, 500 psia) is within the design temperature range for the skirt.

The throat temperature is less sensitive to P_c than is the skirt temperature and behaves more as expected. Although the 20% cooling, 500 psia operating point is shown as exceeding the design temperature, this is not a serious limitation to this design. Because the life-limiting stress condition occurs during the start transient, the design temperature can be increased by making the throat material thinner.

III, A, Activities for Ambient Temperature Propellants (cont.)

The maximum wall temperature in the regeneratively cooled chamber section behaves as expected with the temperature increasing slightly with chamber pressure. Since the film coolant is injected downstream of this section, the measured surface temperature is almost completely independent of the film coolant percentage over the range of values tested.

The effect of varying overall thruster MR from 3.0 to 5.0 has a significant influence on both throat and maximum skirt temperatures at a given percent film cooling flow. This is to be expected. For a given coolant percentage, the absolute quantity of fuel used as film coolant decreases rapidly as the MR increases. Operating at a MR = 5.0 with 30% film cooling gives the same coolant flow as does a MR = 3.0 with 20% film cooling. This is borne out by the temperature data which show these operating conditions to be very similar as far as chamber cooling is concerned.

Quite interestingly, the temperature of the film-cooled portion of the chamber does not vary significantly with the coolant inlet temperature. What apparently is happening is the beneficial effect of lowered coolant temperature is largely offset by the increased mixing resulting from the lower injection velocity of the cold coolant. There is a one-to-one correspondence between coolant temperature and wall temperature in the regeneratively cooled chamber section, which is as expected.

The general conclusions which could be drawn from the above are that this chamber design is not overly sensitive to either chamber pressure of H_2 inlet temperature but will require more than the minimum 20% film cooling if operation at high mixture ratios (>5) is expected for more than a few hundred milliseconds.

III, A, Activities for Ambient Temperature Propellants (cont.)

Figure 18 provides a comparison of the predicted transient temperatures in the copper-lined hydrogen convectively cooled combustion chamber region with gas-side and backside thermocouple measurements from Test 020. Also shown in this figure is a comparison of predicted and measured coolant temperature rise during the first second following ignition. Although the predicted transient responses are similar in character to the measured response, they are off somewhat in absolute value. Posttest disassembly of the hardware indicated the error in the coolant temperature transient resulted from the measuring thermocouple being improperly located. Instead of being in the high velocity coolant stream, the thermocouple junction was located in a recirculation area. As a result, it had lower response and gave an erroneous transient.

The maximum temperature difference across the wall (350°F) is attained during the heating transient between 0.3 and 0.4 sec into the firing. This confirms the computer prediction of a high thermal gradient early in the firing when starting with a cold chamber.

Maximum steady-state copper temperatures range between 600 to 650°F compared to a predicted value of 590°F. Steady-state backside temperatures of 325°F compare to predicted values of 380°F. The steady-state through the wall gradient of 300°F compares with a predicted value of 210°F. Based on the measured wall ΔT being larger than predicted, it might be suspected that the heat flux to the wall is larger than the value found in the Task VIII testing on which the analysis was based. This is not substantiated, however, by the coolant temperature rise data. The measured coolant temperature rise of 130°F is close to the predicted value of 120°F, showing the average flux to the chamber about equal to the Task VIII flux. One possible explanation for the discrepancy is that the thermocouples are not all brazed uniformly and that, as a result, some are in better and more uniform contact with their surroundings than others. This can be evaluated with the firing of the SN 2 film-cooled chamber.

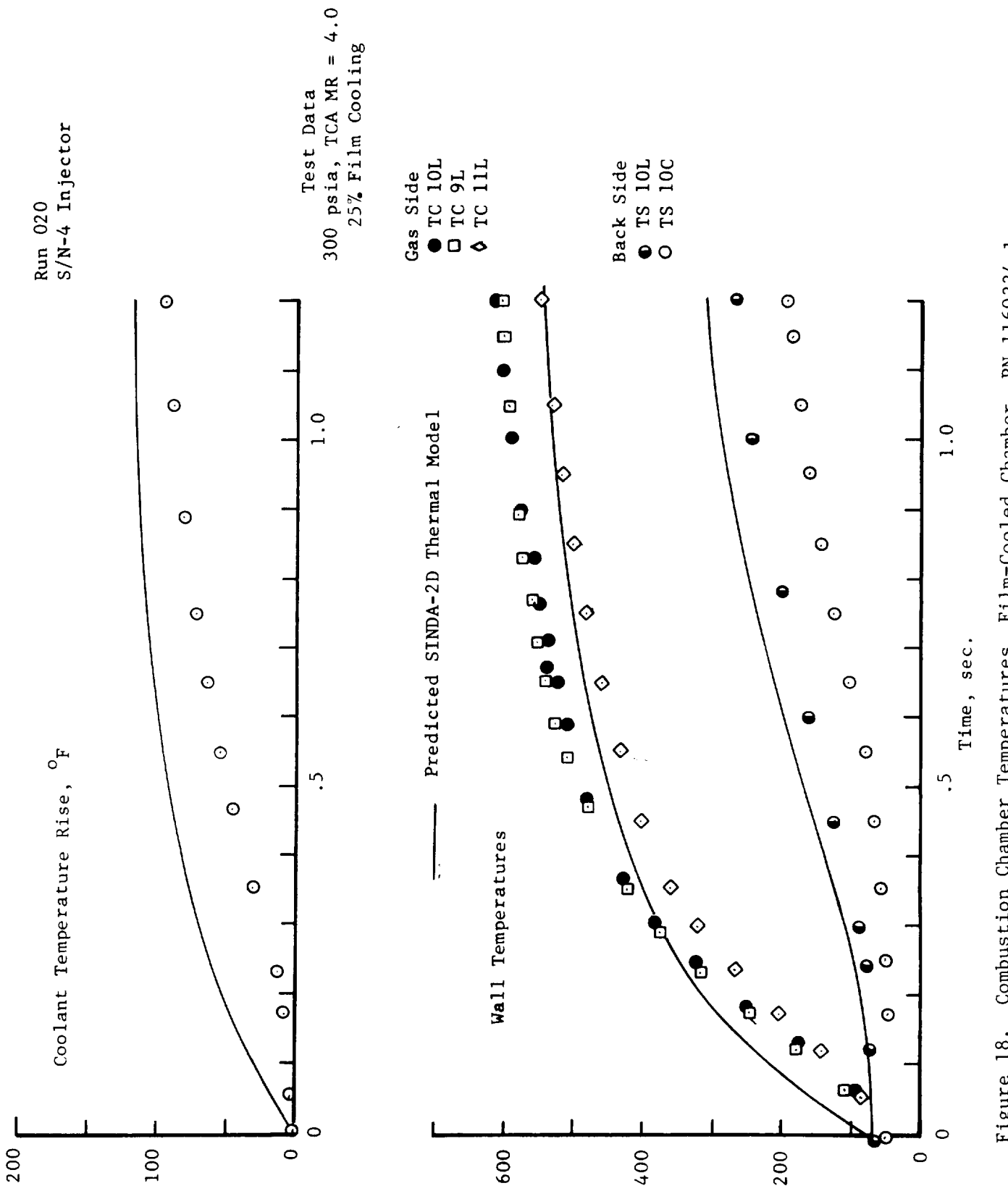

Figure 18. Combustion Chamber Temperatures, Film-Cooled Chamber, PN 1160334-1

III, A, Activities for Ambient Temperature Propellants (cont.)

The heat transfer coefficients derived from the transient heating of the thin wall film-cooled steel nozzle in Test 015 are shown in Figure 19. These coefficients are higher than the values obtained by the usual prediction methods noted but in better agreement with the model which uses local film mixture ratios. The nozzle mass velocity ρV is obtained from the two-dimensional flow conditions near the edge of the boundary layer for an axisymmetric Rao nozzle using the method of characteristics. Figure 20 presents the nozzle film cooling effectiveness for the same test. The effectiveness is based on measured steady-state wall temperatures corrected for radiation losses and computed on the basis that the entrained film and core flow exist in an assumed concentration distribution which is in an equilibrium chemical state. The entrainment multiplying factor (discussed in Report 14354-Q-3) indicates the mixing at the coolant injection station is three to four times greater than should be expected for optimum injection in a nonaccelerating, nonturning, nonreacting situation. The high initial parameter suggests improved coolant injection methods could bring about further reduction in the required film cooling flows and higher engine performance.

8. Task X - Pulse Testing

During this report period, the constant temperature anemometer system to be used for pulse testing on Task X was checked out. Two transducers were successfully calibrated in oxygen and two were successfully calibrated in hydrogen. The calibrations were accomplished in the test circuit with each anemometer in the correct position for pulse flow. The calibrations were made with ambient temperature propellants in a five-step flow range for the purpose of linearizing the transducer output. Approximately 20 flow points were made on each anemometer. A typical analog output curve obtained during these calibrations can be found in Figure 21, which shows excellent full-scale response of approximately 10 millisec and a minimum overshoot. It is felt that this curve represents the actual flow transient in system during the 10 millisec

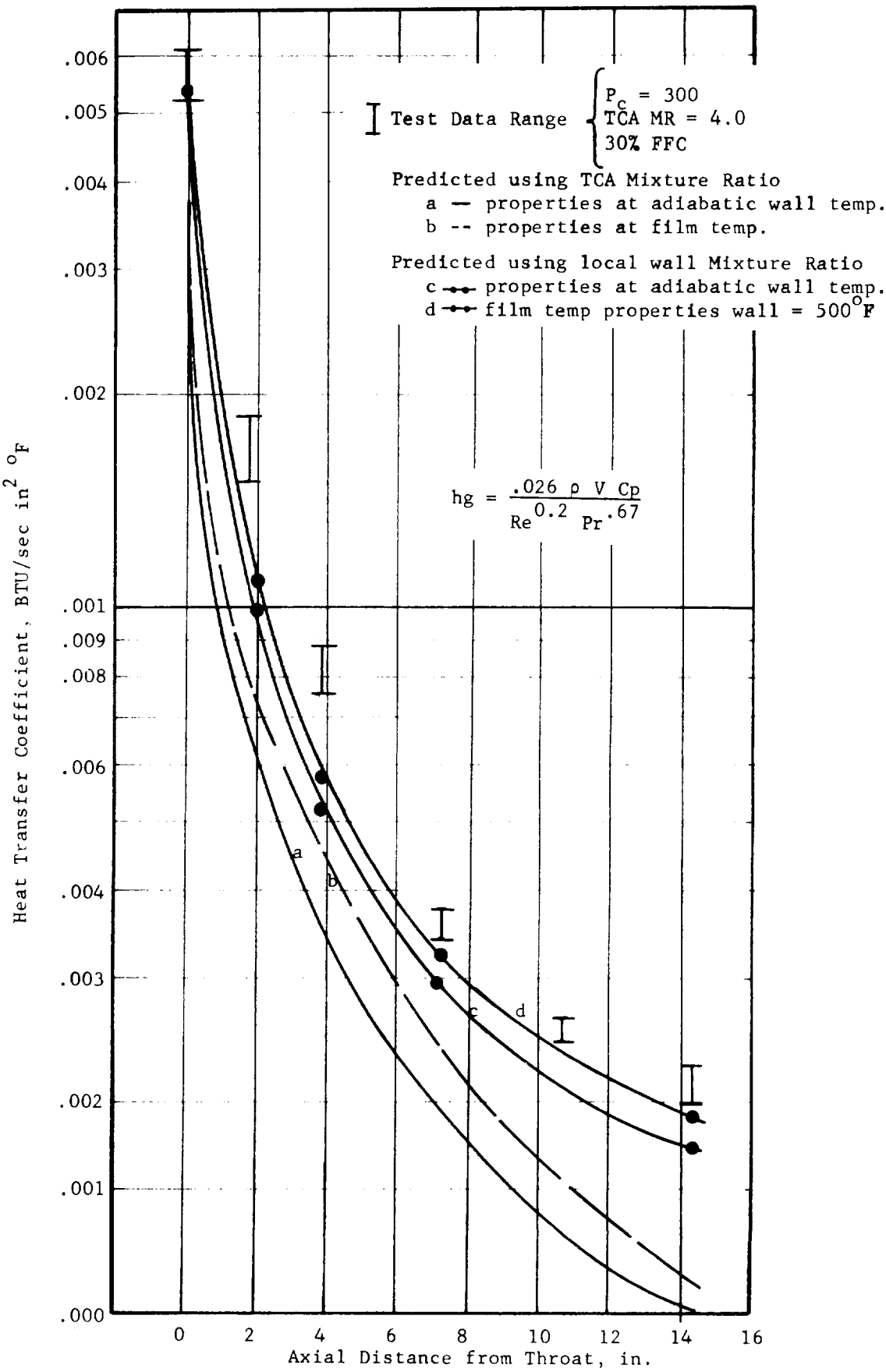

Figure 19. Heat Transfer Coefficients - 40:1 Film-Cooled Nozzle

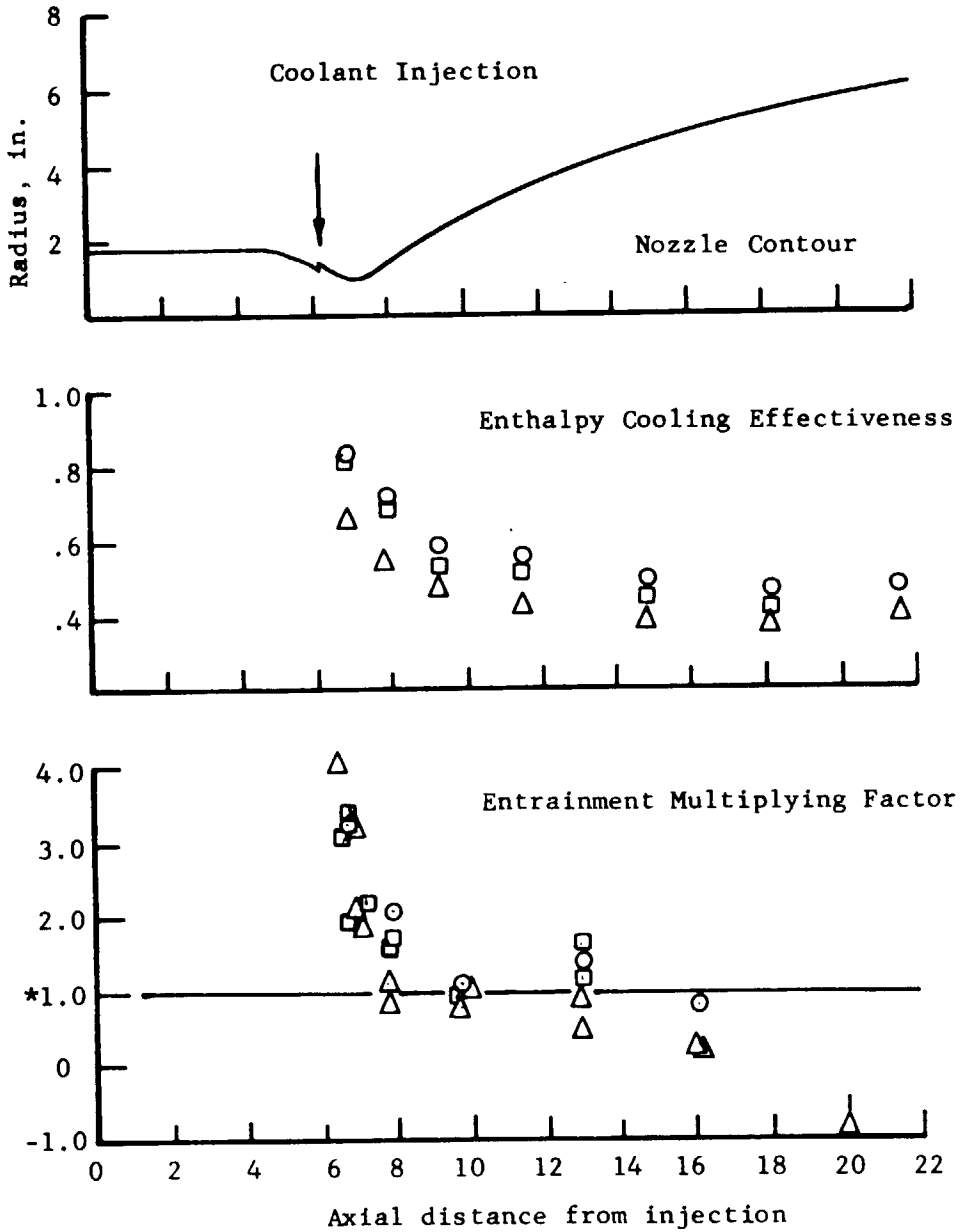

Data P_c = 300 MR = 4.0

Injector SN-5A I Triplet

	% Fuel film cooling	$\frac{\text{Vel. Cool.}}{\text{Vel. Core}}$ +
○	30	1.17
□	25	.87
△	20	.77

+based on equivalent continuous slit height = .024 in. Actual coolant injector 120, .040 x .040 channels.

*1.0 = model predictions neglecting combustion turbulance, nozzle contour, flow acceleration and injector effects.

Figure 20. Cooling Effectiveness and Entrainment Factor, Film-Cooled 40:1 Nozzle

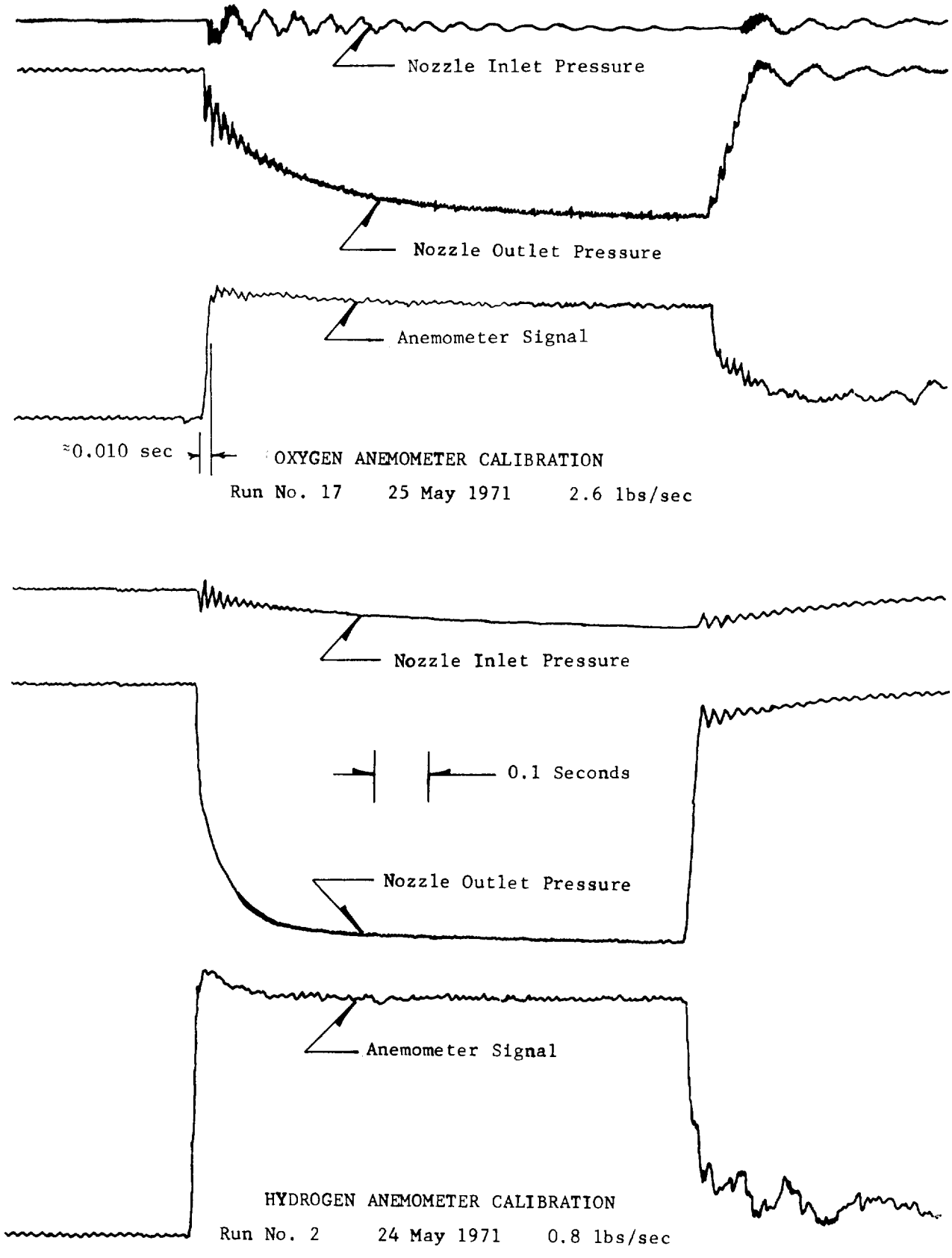

Figure 21. Anemometer Response and Calibration for Pulse Testing

III, A, Activities for Ambient Temperature Propellants (cont.)

valve opening and closing. During the calibrations, two anemometers' filaments were lost while hydrogen flow checks were being accomplished. One filament appeared to be defective and the other failed at its solder joint. The calibration technique utilizing a critical nozzle immediately upstream of the anemometer yields a higher initial pressure and thus a more severe initial flow environment than will exist during the actual pulse testing with the 17 cu ft accumulator between the critical nozzles and the anemometers. In addition, one anemometer was damaged during installation into the propellant line. To solve these problems and to produce a less fragile transducer, four additional anemometers will be supplied by the vendor. These new transducers will have the hot film sensor 0.020 in. in length rather than 0.040 in. in length with the filament standoff probes shorter and stronger than the units tested. These modifications will improve the sensor strength by a factor of at least four. A special mounting/protector tool will be attached to each new transducer which will prevent any further installation or handling problems. These new transducers will be delivered during the week of 14 June 1971.

A test plan for pulsing tests was prepared and submitted for NASA approval.

B. HIGH P_c TASKS IN REDIRECTED PROGRAM

1. Task XXII - Design of Injector for Low Temperature Propellants

Design of a new injector manifold suitable for pulsing with low temperature propellants was completed. This design is shown in Figure 22. This new manifold configuration incorporates the most successful features of both high and low P_c injector designs as established from the extensive manifold cold flow studies which were conducted in the earlier tasks. The new manifolding is designed to accommodate a bonded platelet stack containing

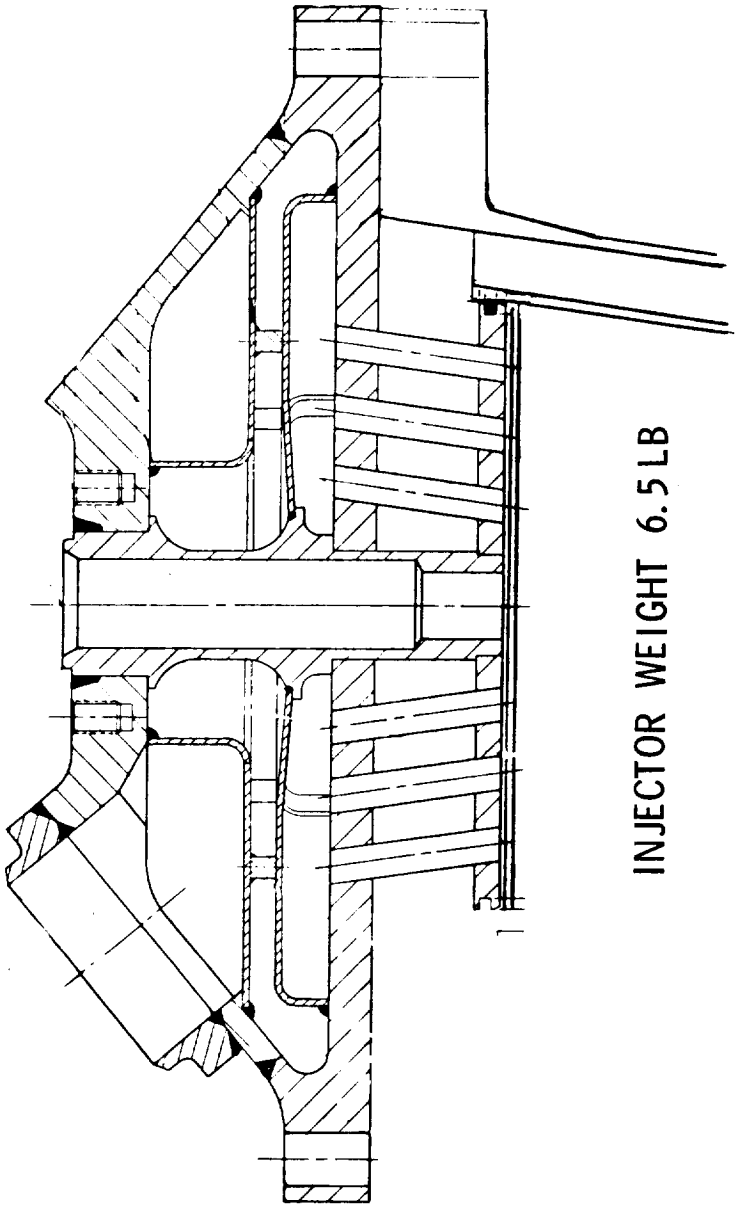

Figure 22. 72-Element Premix Injector Manifolding

III, B, High P_c Tasks in Redirected Program (cont.)

72 injector elements. The final pattern to be applied can be either the "I" premix triplet, a premix triplet, or any other improved pattern which can be generated by the bonded plate stack design approach. This design also allows the oxidizer orifices or tubes to be made as individual high recovery sonic venturis to give a degree of passive mixture ratio control to the injector. A second -2 assembly provides oxidizer tubes oriented in an axial rather than a canted direction. These respective designs are suitable for use in either conical or cylindrical combustion chamber contours. Design goals for this third generation design were to reduce both injector weight and volume, while at the same time providing near ideal propellant distribution through all 72 elements. The structural design criteria (per the contract requirements to obtain data at chamber pressures up to 500 psia) are as follows:

Chamber pressure, P_c	500 psi (nominal)
Oxidizer manifold pressure, P_{oj}	600 psi (nominal
Fuel manifold pressure, P_{fj}	600 psi (nominal)
Proof	700 psi

Propellant temperatures to the injector are 375°R for the oxidizer and 250°R plus coolant jacket temperature rise for the fuel.

Comparison of the Task I and Task XXII injectors is as follows:

	I	XXII
ΔP fuel, psi	42	40
ΔP oxidizer, psi	51	40
Weight, lb	10	6.5
Volume, $in.^3$ - Fuel	30	7.5
Oxidizer	30	18.0

III, B, High P_c Tasks in Redirected Program (cont.)

For flight designs, an additional two pounds of weight could be eliminated if the design pressure were reduced to correspond to the nominal 300 psia P_c rather than 500 psia and the injector were welded rather than bolted to the thrust chamber. The use of materials of higher strength than CRES 304 would provide some additional weight savings.

The propellant flow distribution in the oxidizer circuit, as determined from cold flow tests using GN_2, has been found to deviate less than 2% from the mean value. These data are shown in Figure 23.

2. Structural Analysis

a. Design Criteria

(1) Factor of Safety

A 1.25 factor is applied to all nominal pressures to produce limit design loads.

(2) Failure Criteria

The Huber-Von Mises-Hencky yield criterion was used as a basis for establishing the structural adequacy of the High P_c injector. This criterion states that, when the effective stress exceeds the uniaxial yield strength of an elastic material, yielding will occur. The effective stress is computed from the following expression:

$$\sigma_{eff} = \{1/2\ [(\sigma_1 - \sigma_2)^2 + (\sigma_1 - \sigma_\theta)^2 + (\sigma_2 - \sigma_\theta)^2]\}^{1/2}$$

The margin of safety is:

$$M.S. = \frac{\sigma_{allow}}{\sigma_{eff}} - 1$$

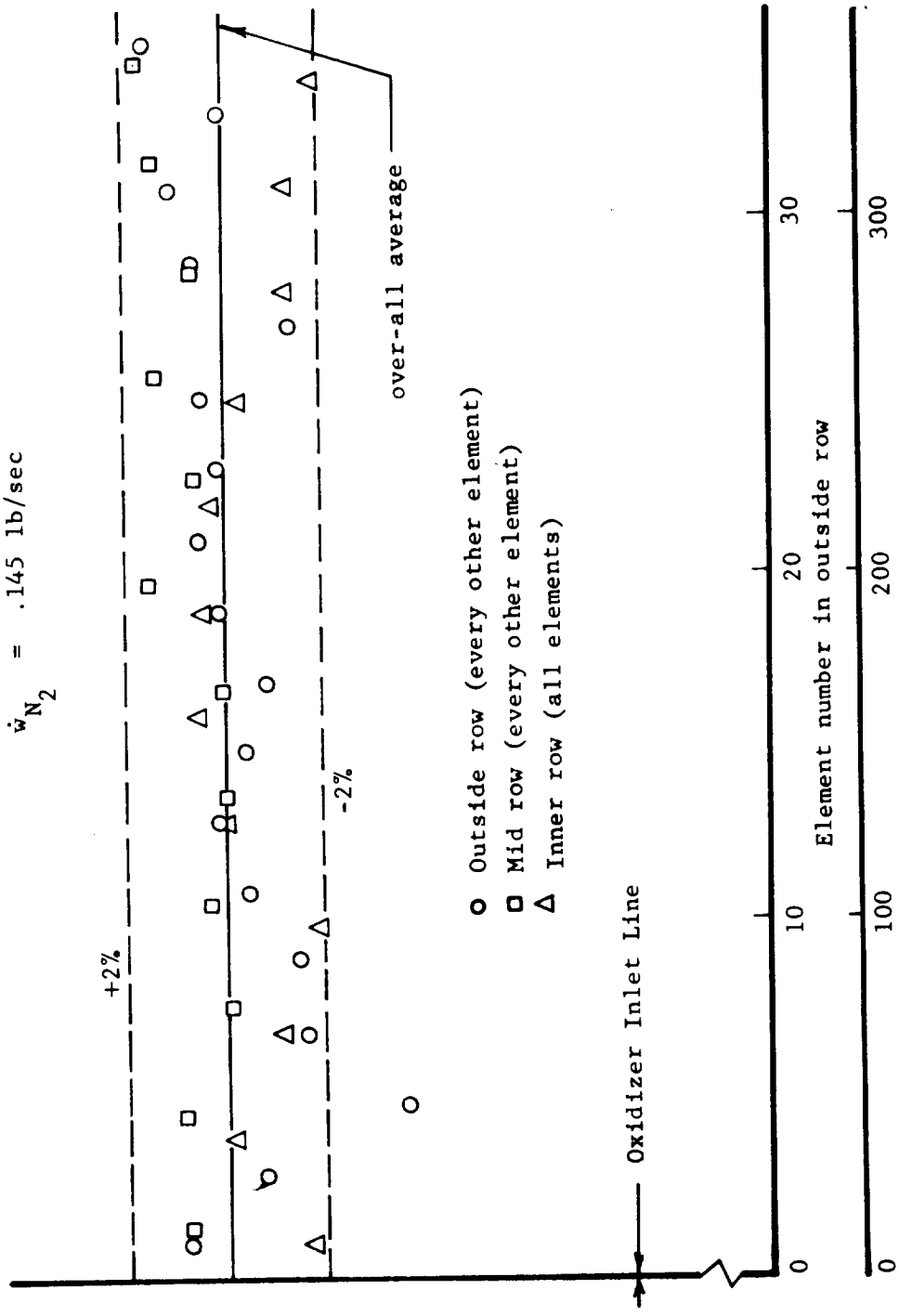

Figure 23. Oxidizer Flow Distribution Premix Injector with GN_2

III, B, High P_c Tasks in Redirected Program (cont.)

where σ_1 = principal stress in the radial direction
σ_2 = principal stress in the Z direction
σ_θ = circumferential (hoop) stress
σ_{allow} = uniaxial material allowable

Fatigue life of a component is established by comparing the total maximum strain to an S-N curve of the particular material.

b. Materials

All components are annealed Type 304 stainless steel except the face platelet stack which is annealed Nickel 200.

Type 304 Stainless Steel

F_{tu} = 75,000 psi
F_{ty} = 30,000 psi
E = 29.0 (10^6) psi
μ = 0.30
α = 9.2 (10^{-6}) in./in./°F

Nickel 200

	R.T.	600°F	1200°F
F_{tu}	67,000	66,200	21,500
F_{ty}	21,500	20,300	10,000
E	30 (10^6)	--	--
μ	0.3	0.3	0.3
α	7.4 (10^{-6})	8.0 (10^{-6})	8.7 (10^{-6})

III, B, High P_c Tasks in Redirected Program (cont.)

3. Method of Analysis

The structural components of the High P_c injector was analyzed as a figure of revolution loaded by pressure. To facilitate the analyses, the injector geometry was introduced to the AB5U Computer Program. This program is a finite element stress analysis of axisymmetric and plane structures.

The model shown in Figure 24 was introduced to three different loading conditions which correspond to the three possible operating modes. These modes are: (1) proof pressure in the chamber with the injector used as a closure (no ΔP across the face or injector plate), (2) oxidizer lead with full pressure in the oxidizer manifold and zero pressure in the fuel cavity and chamber, and (3) fuel lead with full pressure in the fuel manifold while pressure is zero in the chamber and oxidizer manifold.

In all cases the injector is fixed against axial deflection and rotation at the bolt circle.

The platelet stack attached to the injector face is subjected to rather steep temperature gradients which, in turn, force the material well into the plastic range. The maximum thermal strains are determined by:

$$\varepsilon_{max} = \alpha \Delta T$$

where: α = coefficient of thermal expansion

ΔT = temperature gradient

This relationship is for a plate that is fully restrained while exposed to a temperature gradient.

Fatigue life of the face is based on a comparison between the calculated maximum thermal strains and an empirically derived S-N curve for the material.

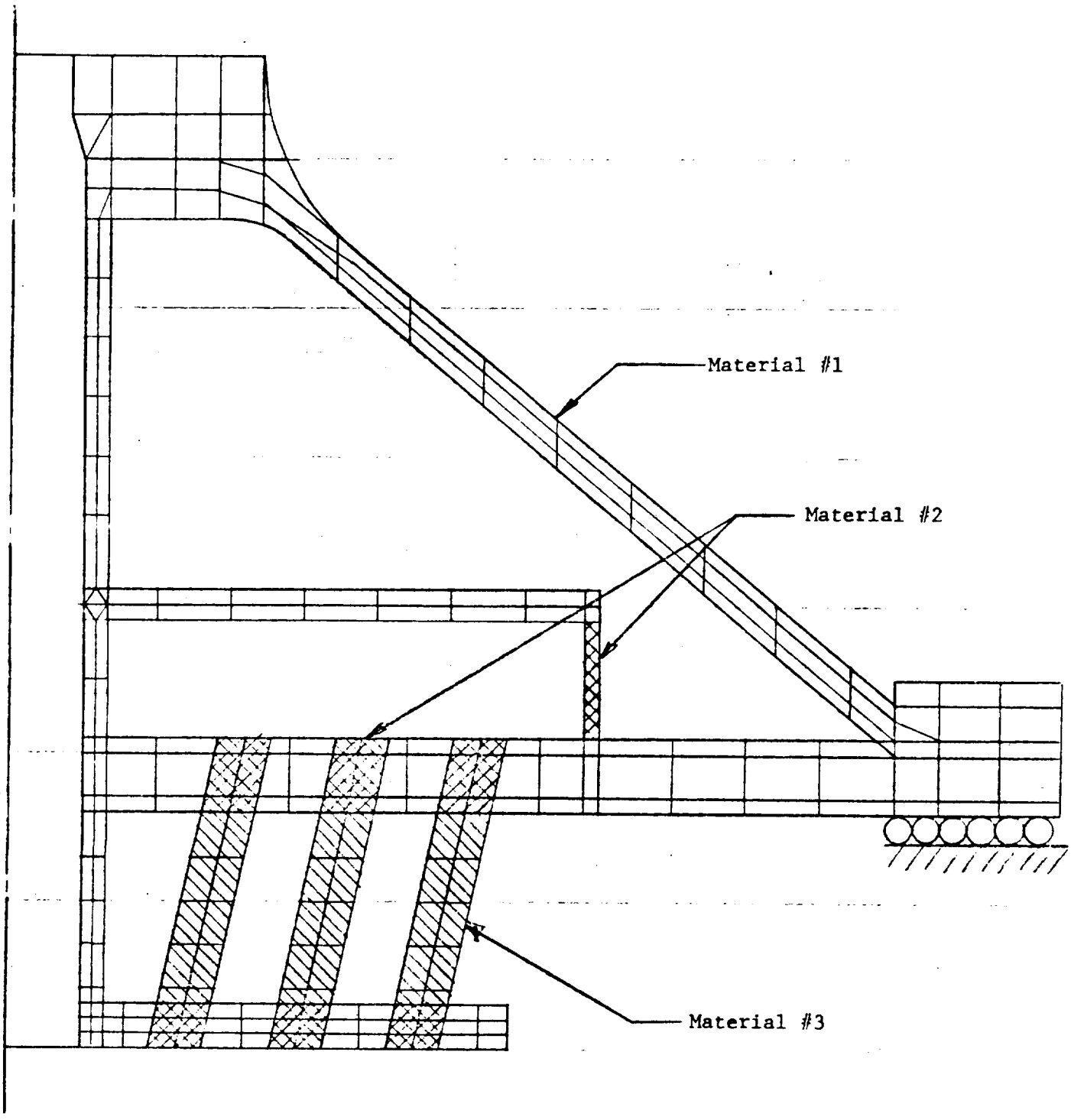

Figure 24. Computer Representation of the High Chamber Pressure Injector

III, B, High P_c Tasks in Redirected Program (cont.)

4. Results of Analysis

a. Pressure Strains

The design shown in Figure 22 operates in the elastic material range throughout. The maximum stress at the most severe proof or overpressure conditions is 83% of the material yield strength at 70°F. Under normal 300 psia P_c cyclic operation, maximum stress is 42% of yield (0.044% strain), thus ensuring a pressure cyclic life $>10^6$.

b. Thermal Strains

The orifice pattern on the face is such that when the fuel impinges on the oxidizer a fan-shaped flame is produced. This flame in turn impinges on the Nickel 200 platelet face, causing a local surface hot zone. Thermocouples located on the injector face during firings with various element configurations have shown that the local face temperature can be maintained at fuel temperature plus 200°F to fuel temperature plus 800°F, depending on the pattern design selected.

The analysis assumes the cold side of the bonded nickel face platelets is stressed in tension while the hot side is in compression. The backside of the platelet face is not only at propellant temperature but is also held at approximately zero strain by the relatively heavy steel face plate. The strain on the hot face for the fully restrained condition then is:

$$\varepsilon_{max} = \alpha \Delta T$$

III, B, High P_c Tasks in Redirected Program (cont.)

c. Fatigue Life

Figure 25 shows the relationship between total strain and fatigue life for Nickel 200 at 70°F and 600°F. Both curves fall on one line, reflecting the material's insensitivity to temperature in this range. However, for temperatures in excess of 600°F, the mechanical properties fall off rapidly and a significant deterioration of fatigue life can be expected. A data point from a RPL test at 1400°F and an estimated fatigue life curve at 1400°F is also shown in Figure 25 and can be used to bracket the fatigue life for temperatures above 600°F.

ΔT	ε_{max}	N_f
0	0	∞
200	0.148%	$>10^6$
400	0.308%	50.0 (10^3)
600	0.480%	11.0 (10^3)
800	0.655%	5.6 (10^3)
1000	0.850%	(0.9 to 3.0)(10^3)

Figure 26 shows the relationship between fatigue life and temperature gradient across the face.

5. Task XXIII - Injector Fabrication

During this report period, machining was completed for components for two injector assemblies. The first unit was assembled via standard brazing and electron beam welding techniques. Figure 27 shows the injector before the face plates are bonded. Figure 28 shows the same injector after bonding of the face platelets containing the modified "I" fuel pattern. Welding of the oxidizer inlet lines was completed after face bonding. The second set of components is being held in a disassembled state pending final assembly and checkout of the first unit.

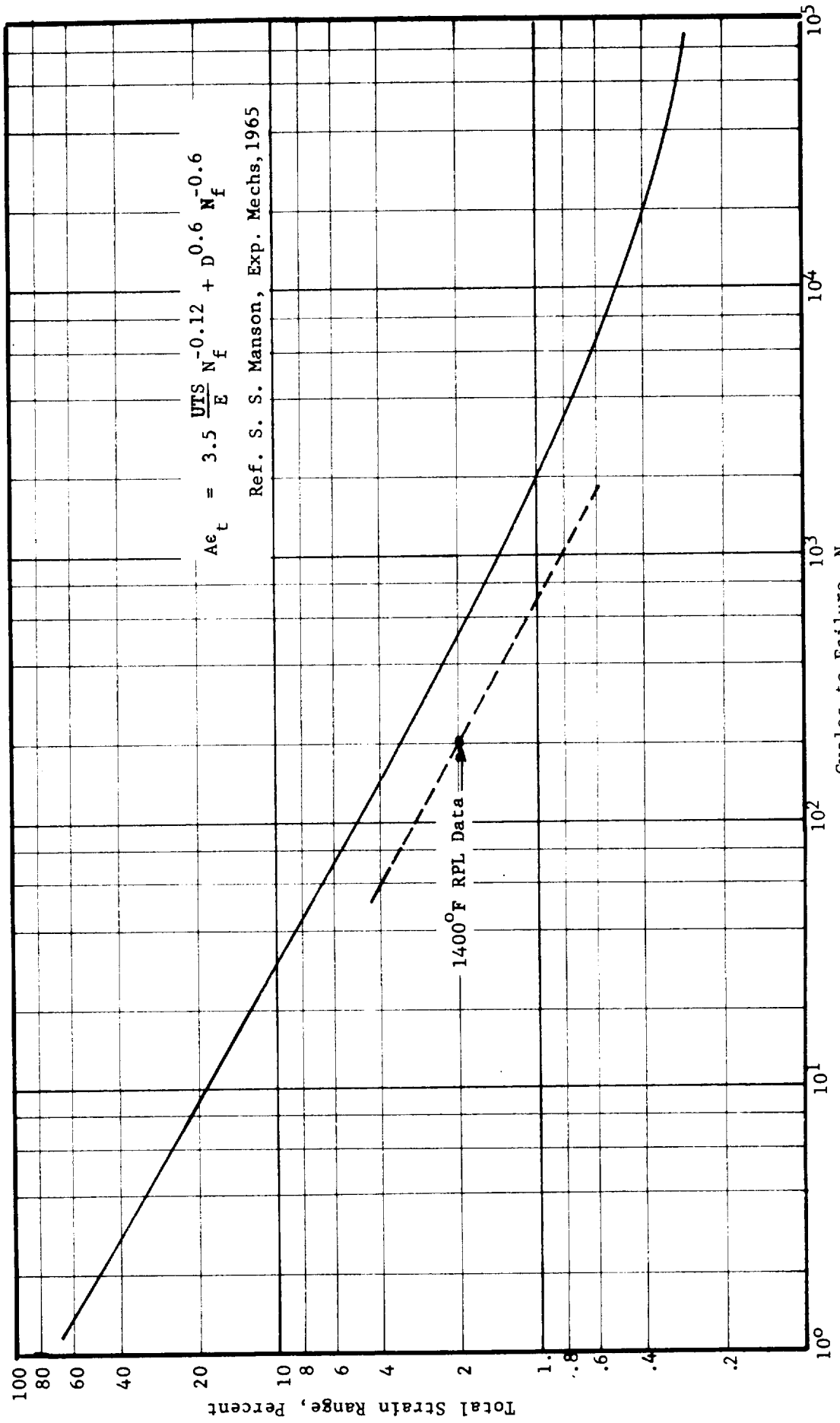

Figure 25. Fatigue Life vs Total Strain Range for Nickel 200 at 70°F and 600°F

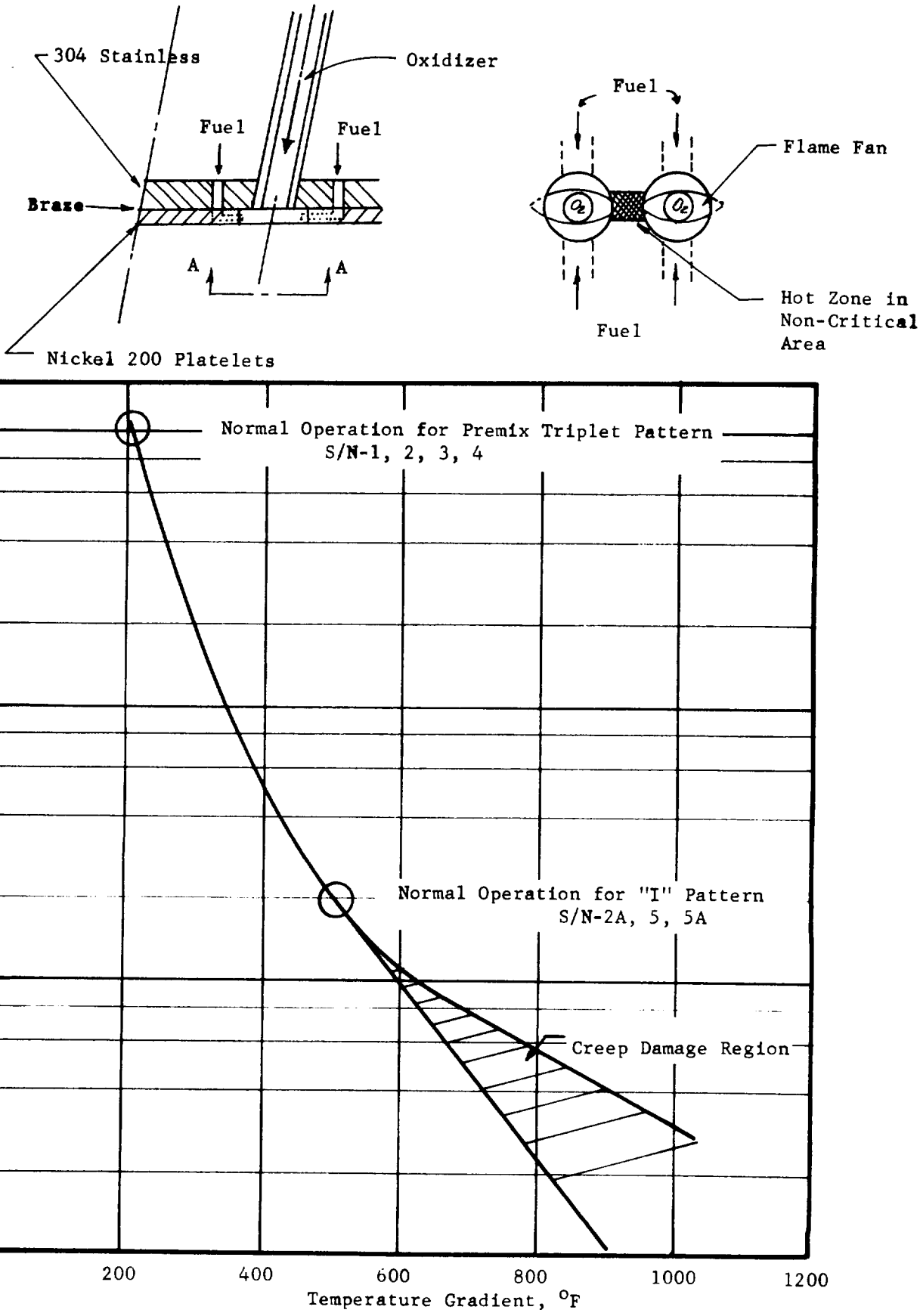

Figure 26. Fatigue Life vs Temperature Gradients for Platelet Injector Face

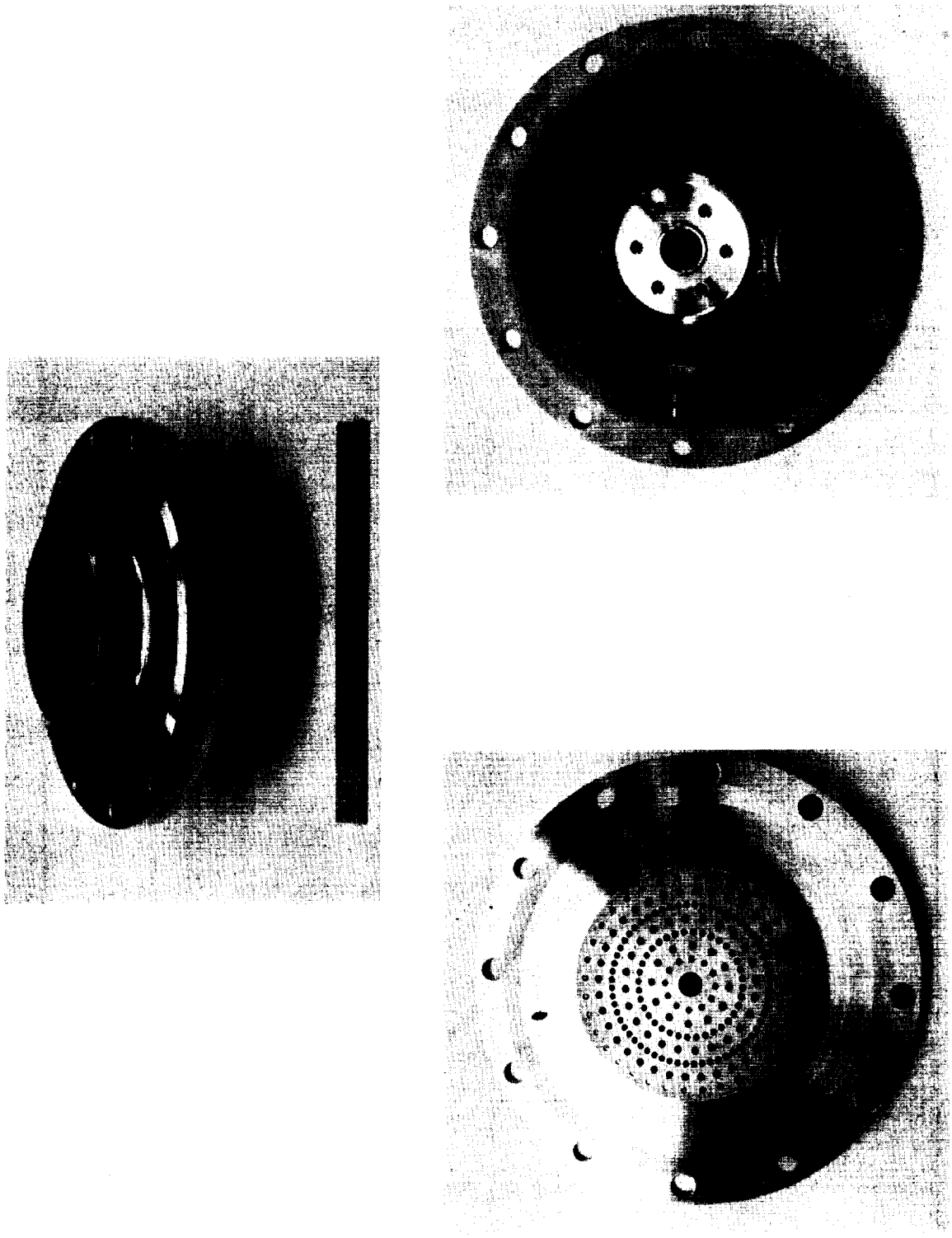

Figure 27. 72-Element Injector Manifolding Before Face Plate Bonding

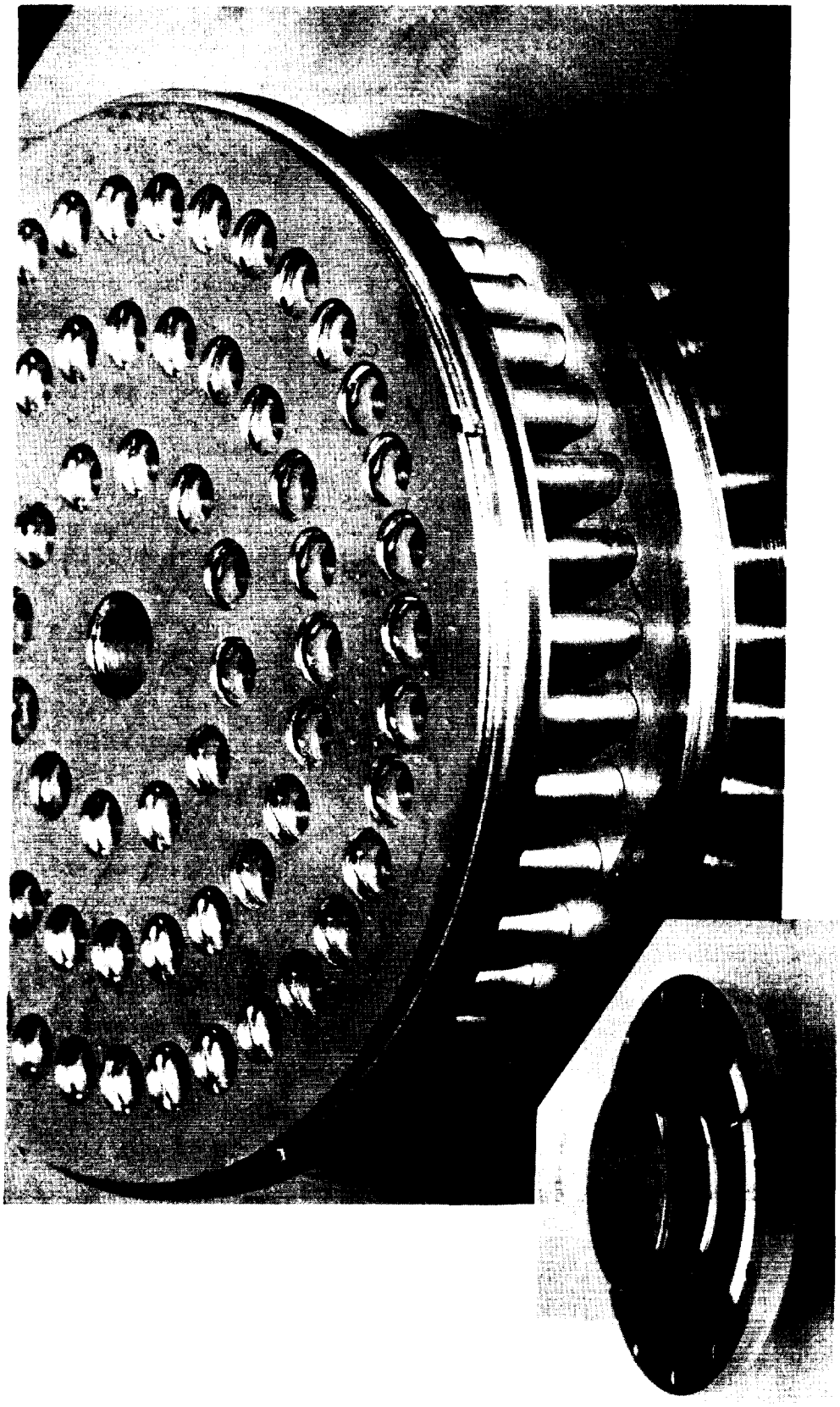

Figure 28. 72-Element Premix I-Triplet Injector

III, B, High P_c Tasks in Redirected Program (cont.)

6. Task XXIV - Cooled Chamber Analysis and Design

The technical objectives of this task are as follows:

(1) Re-optimize the manifolding and coolant channel geometry of Task III film-cooled and regeneratively cooled chamber designs to reflect the revised propellant temperature schedules.

(2) Design a film-cooled nozzle skirt suitable for use with either above design which is capable of operation at temperatures in excess of 2000°F.

(3) Generate one new chamber design in which primary emphasis is placed on achieving minimum weight and the ability to withstand long exposure to a 2000°F reentry heating environment.

Design modification in the first objective category involves a reduction of both manifold and coolant channel cross-sectional areas to be compatible with the higher density propellants. Design modifications are also being made to integrate data acquired in fabrication, cold flow, and hot fire tests conducted in the first ten program tasks. Each of these new designs also will evaluate nonrestricting manifolds which accommodate relative movement of the thermally contracting manifold and expansion to the hot inner wall. Activities in this task have proceeded to the point where: (1) the channels have been resized for both designs and optimized for the high reentry temperature design; (2) structural analyses of these designs, including the nonrestricting manifolds, are now in progress; and (3) the high temperature skirt materials evaluation has been completed.

a. Lightweight, High Temperature Design

In the new lightweight chamber design study, the use of copper is excluded at all locations since the melting temperature of this material is less than the 2000°F reentry heating condition. The designs being

III, B, High P_c Tasks in Redirected Program (cont.)

investigated (as shown in Figure 29) build off the successful fabrication and test experience of the nickel/steel film-cooling rings used in Task VIII and the film-cooled Haynes 188/stainless steel 40:1 nozzles demonstrated in Task IX.

Thermal Analysis

The new design employs a parallel-flow dump cooling arrangement in a conical 5.5-in.-L' combustion chamber. Based on Task IX test results, 20% of the fuel is used to convectively cool a 3-in.-long slotted and bonded ring which may be either of nickel or a high-strength nickel alloy. The coolant discharging from the ring is capable of film cooling the nozzle to any area ratio. A smaller amount of additional film cooling is provided from the injector face to obtain the desired cyclic life of the ring and coolant pressure drop. Figure 30 shows the results of a comprehensive parametric analysis which optimized the length, materials, number, and size of coolant channels and coolant flow in the convectively cooled section. Nickel is recommended for the film cooling ring because its higher thermal conductivity results in lower temperature gradients. The optimized wall configuration contains 160 coolant channels 0.025 in. deep, 0.030 in. wide, within a 0.080-in.-thick composite nickel/steel wall. The upper left plot in Figure 30 shows the maximum wall temperature at nominal design conditions vs percent face plane injected coolant for various dump ring lengths, with a constant 20% fuel flow through the ring. The maximum gas-side nickel wall temperature for a 3-in. length can be selected to fall between 400°F and 950°F as the face plane coolant is reduced from 10% to 0. The resulting inside-to-outside thermal gradients (which dictate chamber life) correspondingly vary from 300°F at the maximum flow to 660°F at zero face plane coolant injection. The corresponding pressure drop characteristics and injection velocities are shown in the lower two figures. The final selection of face plane cooling will be dictated by cyclic life and pressure drop consideration, which are now being evaluated.

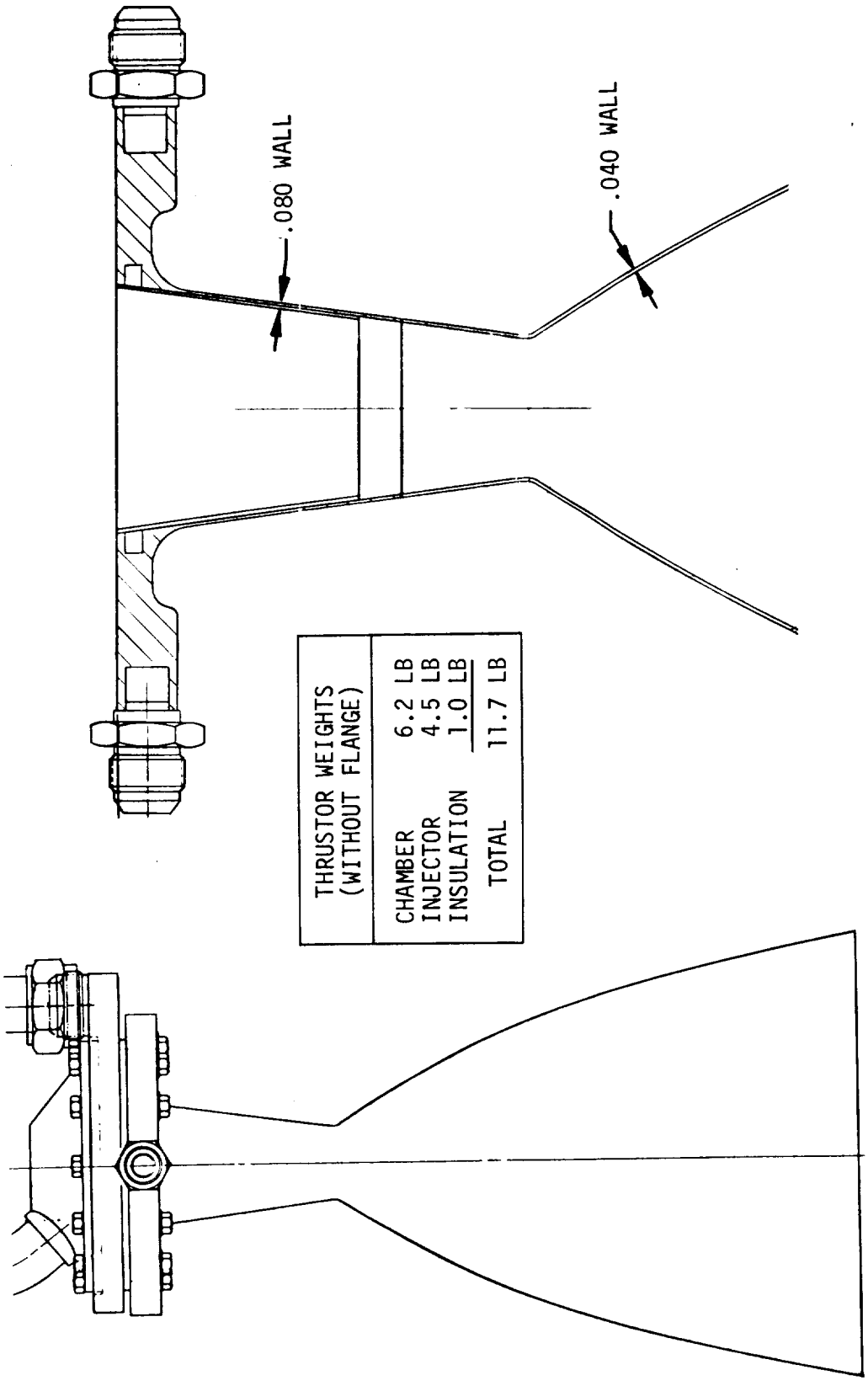

Figure 29. Minimum Weight Film-Cooled Chamber for 2000°F Reentry Heating

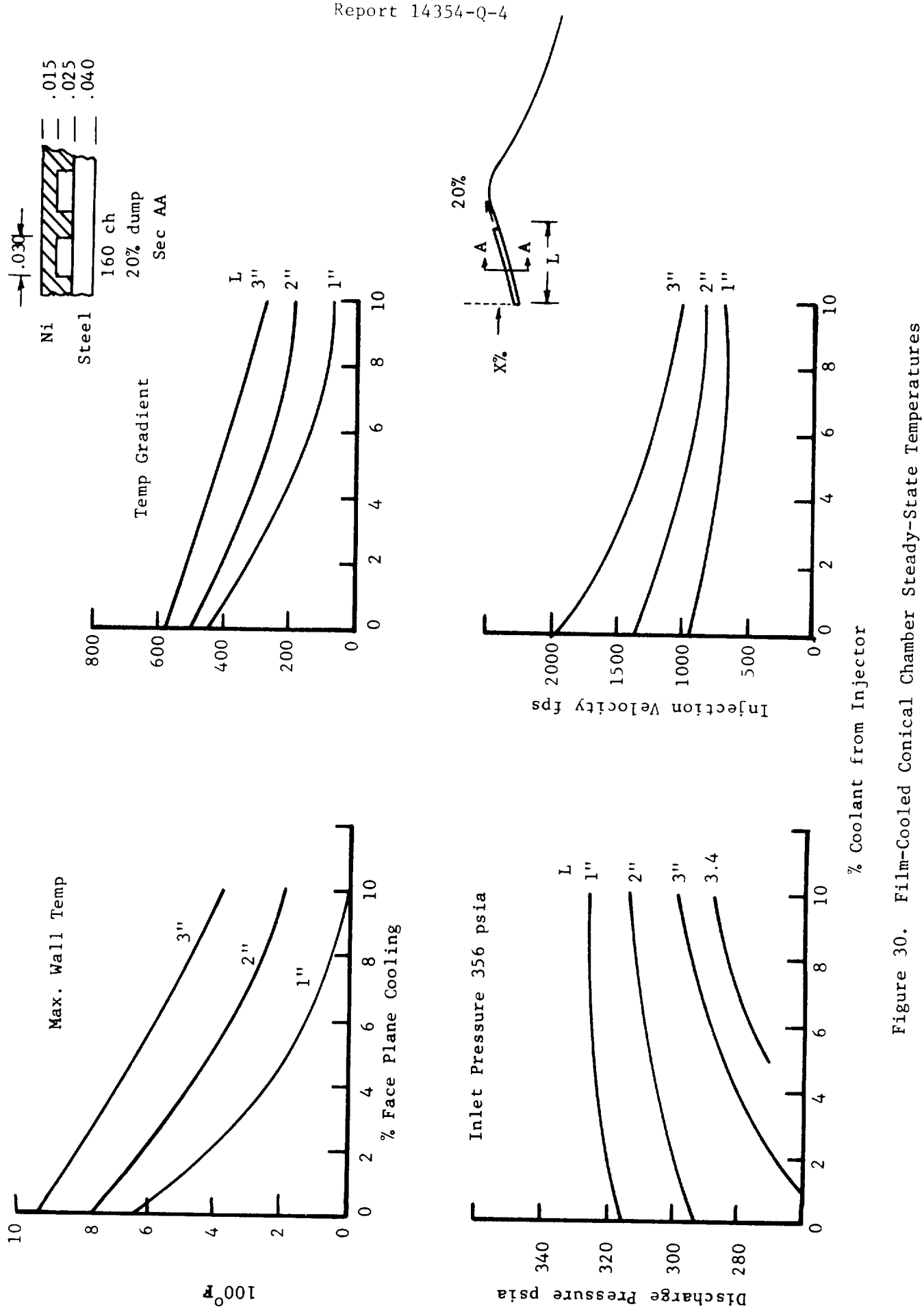

Figure 30. Film-Cooled Conical Chamber Steady-State Temperatures

III, B, High P_c Tasks in Redirected Program (cont.)

The second portion of the analysis, which applies to the region downstream of the dump is shown in Figure 31. This analysis applies to both mono-wall film-cooled designs being considered. This figure provides the basis for the thermal/stress analysis as it contains both the transient and steady-state temperature gradients. The parameters generated in this figure are derived for a nozzle wall which is 0.040-in. thick from the coolant injection point to 40:1 area ratio, using the experimental heat transfer coefficients and recovery temperatures from Test 015 in Task IX. The plot shows axial temperature gradients at steady-state, radial temperature (ΔT max) during transient, and the wall heating rate at eight locations. Maximum throat strains are developed between 0.05 to 0.10 sec after fire switch, however, only when the chamber wall is cold. If the engine is pulsing rapidly and the wall is at near steady-state temperatures, thermal gradients and resulting strains will be reduced considerably. Current structural analyses are being conservatively conducted on the basis of the number of cold starts.

Structural Analysis

The cyclic and creep rupture life of the single wall throat and skirt has been computed based on the experimental temperatures and transient heating rates measured on SN 1 film-cooled chamber in Test 015 of Task IX as shown in Figure 31. This analysis begins at the film coolant injection station, extends through the Haynes 188 throat and 304 stainless steel skirt to an area ratio of 40:1. The life analysis applies to either the conical chamber design or the modified Task III film-cooled design.

Figure 32 shows the effective stress in the throat region where the Haynes 188 alloy is employed. The major stresses are due to the thermal gradient which develops across the wall when the thruster is cold started. A maximum effective stress of 72 ksi is developed in the throat section between 0.05 and 0.10 sec when the thruster is started cold. The major

0.040 in. Haynes/304 Nozzle
MR = 4, 19% Film Cooling

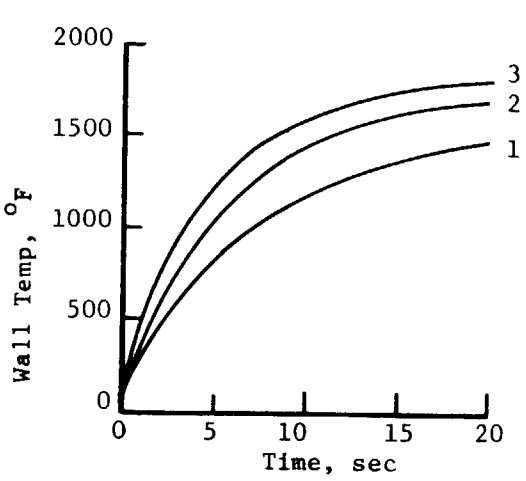

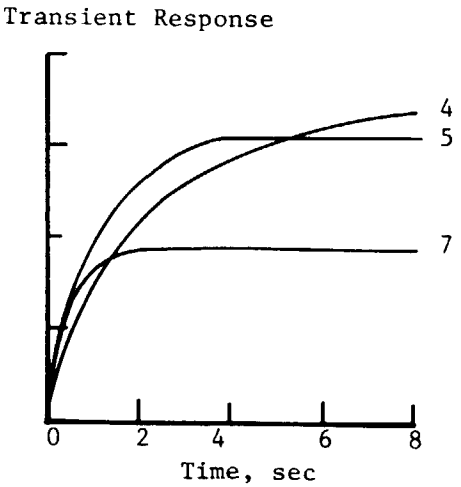

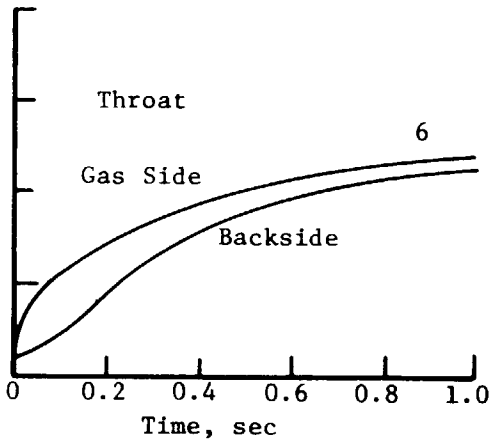

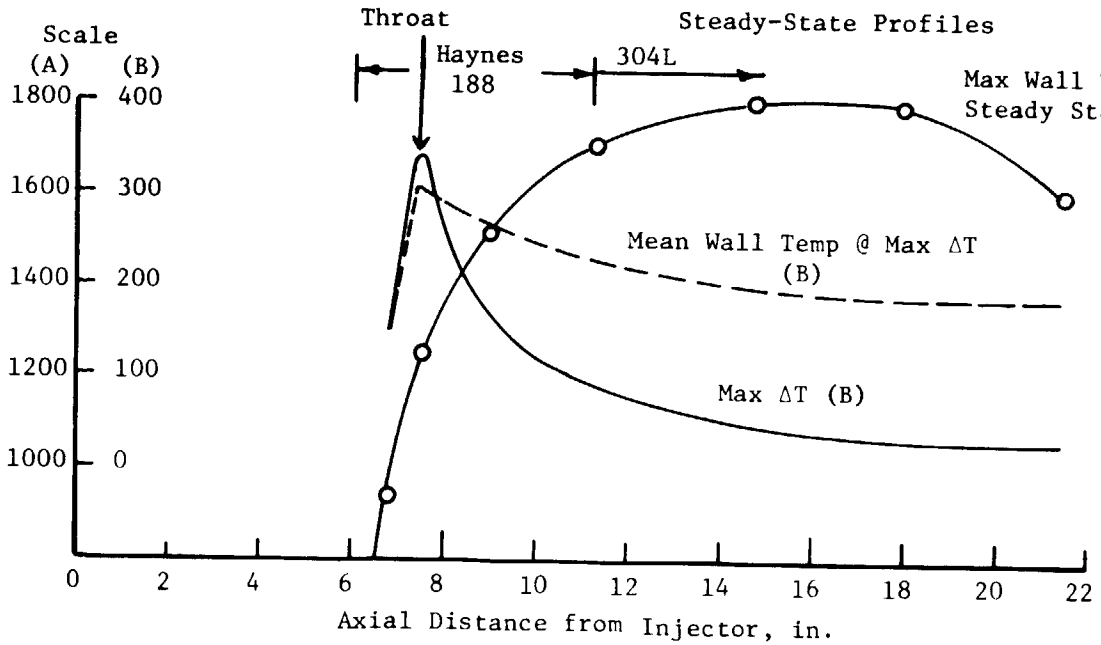

	Axial Dist, in.	Steady State ΔT_{max} °F	Transient ΔT_{max} °F
1.	21.4	1600	30
2.	18.0	1800	34
3.	14.7	1800	42
4.	11.3	1700	96
5.	9.2	1550	152
6.	7.44	1250	340
7.	6.8	955	163
8.	6.2	650	--

Coolant Injection 6.2 in.

Figure 31. Film-Cooled Nozzle Thermal Profiles Based on Data, Test 1680-D03-0A-015

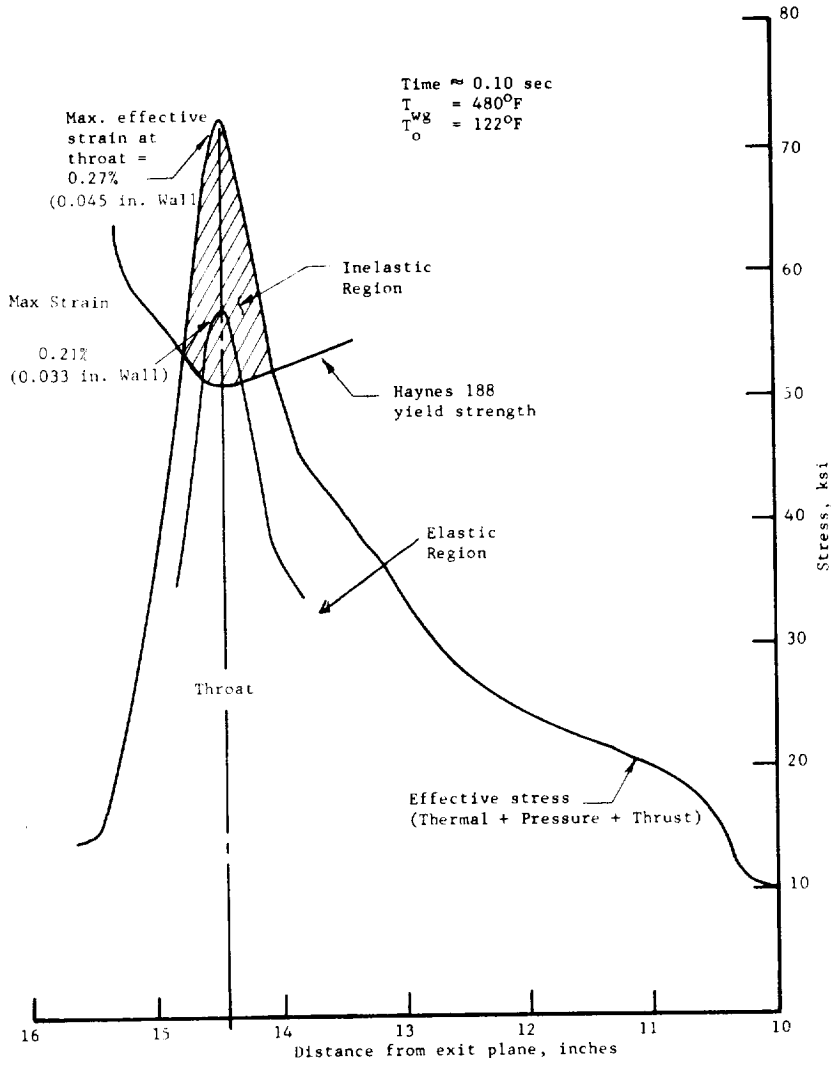

Figure 32. Throat Combined Stress Profile Transient Thermal Stress, 300 psi Chamber Pressure

III, B, High P_c Tasks in Redirected Program (cont.)

component of this stress is due to the radial gradient through the wall. These stresses are actually reduced as the wall is made thinner. The analysis is for a nominal 0.040 to 0.045 in. wall thickness and results in an effective strain of 0.27%. Strains of 0.27% and 0.22% convert to cycle lives of 4.6×10^5 and 1×10^6 for throat wall thicknesses of 0.045 and 0.033 in., respectively, as shown in Figure 33.

The radial temperature gradient decreases as the thruster continues to fire. At steady-state firing conditions (after about 1.0 sec), the remaining structural loads on the nozzle are due to thrust, internal pressure, axial temperature gradients, and whatever side loads or vibrational forces generated by the system. These result in the effective steady-state stress profile shown in Figure 34. The throat stress drops from the transient 72 ksi down to a 5 ksi steady-state value. The 5 ksi compares favorably to an allowable, at temperature, 50-hr creep rupture stress of 40 ksi.

Figure 34 further shows the actual steady-state stresses to be considerably below the 50-hr creep rupture limits of the selected materials throughout the length of the mono-wall portion of the chamber. The high stresses at the 10-in. location are a result of the Haynes 188/304 stainless steel weld joint prior to stress relief.

b. Regeneratively Cooled Chamber Design

The Task VIII test data showed that, to obtain the life goal of 100,000 full thermal cycles with the regeneratively cooled design, would require more film cooling than the film-cooled chamber design. These data and predictions are summarized as follows:

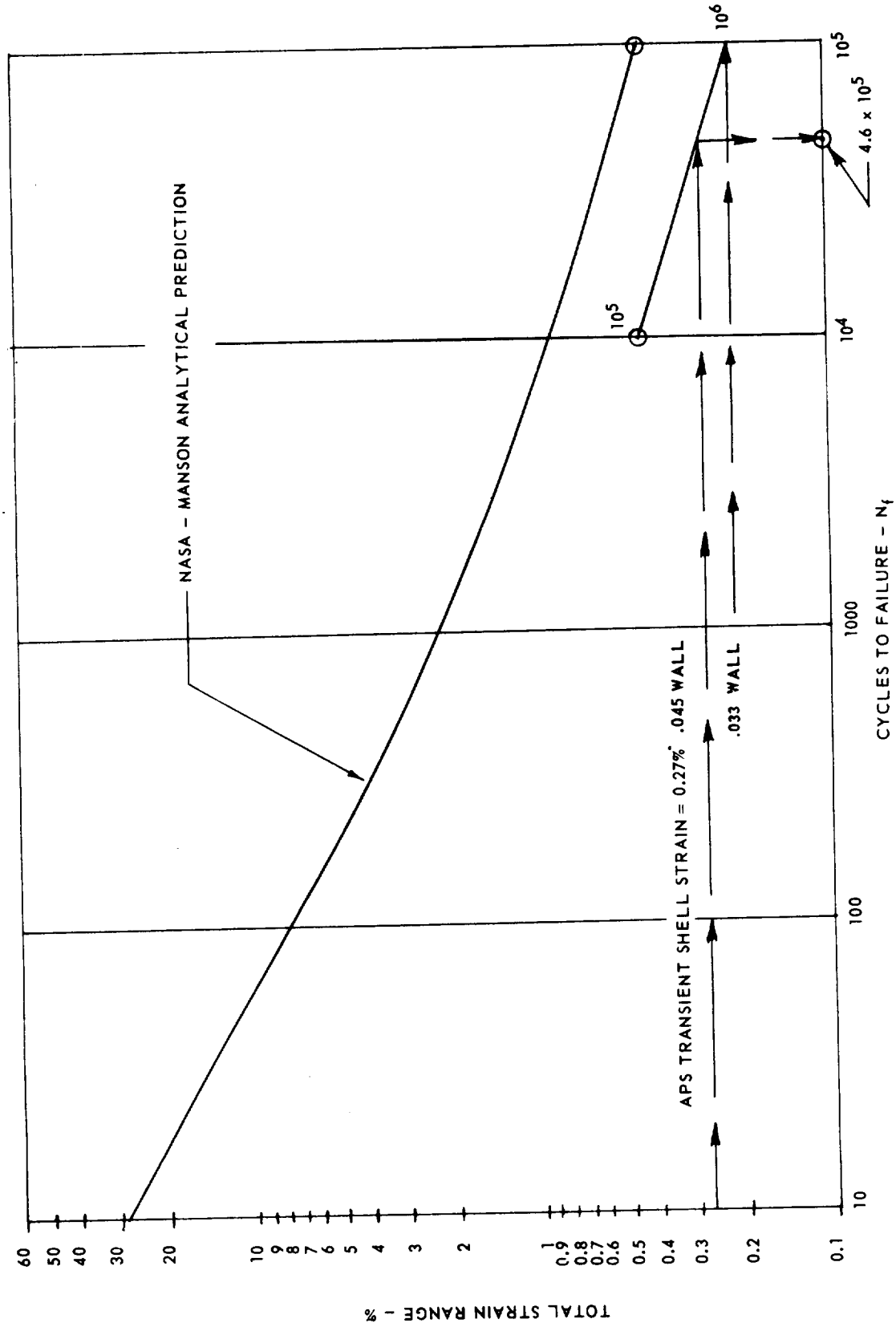

Figure 33. Haynes 188 Fatigue Life - 1000°F

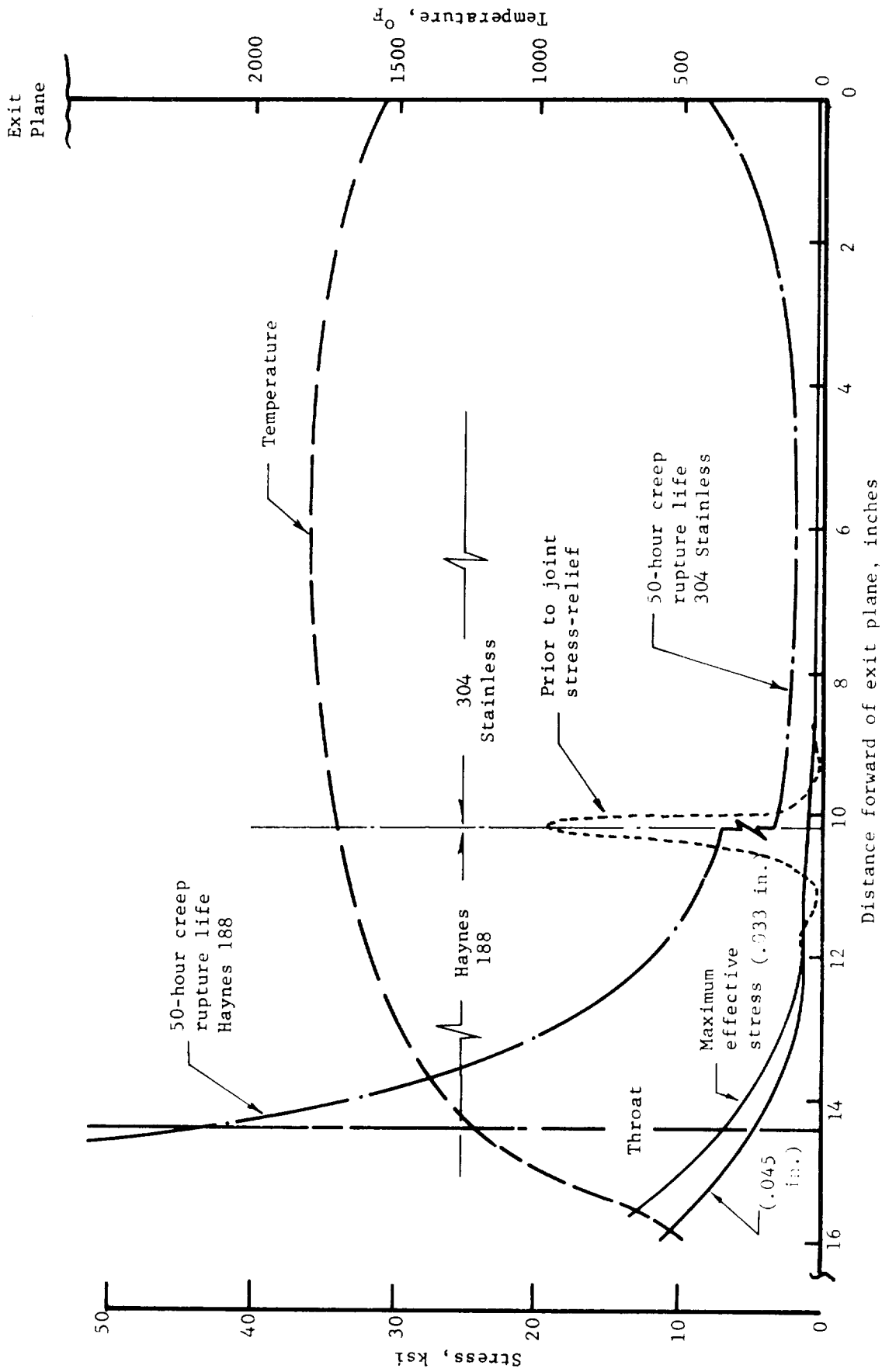

Figure 34. Steady-State Nozzle Stress Profiles, 300 psi Chamber Pressure

III, B, High P_c Tasks in Redirected Program (cont.)

Film Coolant Injection at Face Plane

% FC	T Wall, °F	Heat Flux, Btu/sec-in.^{2}	Projected* $I_{s(vac)}$, sec	Throat N_f (Thermal) Zirconium Copper
0	820	12.0	450	5000
20	800	11.8	440	6000
30	600	8.0	430	13,000

Film Coolant Injection 2.5 in. Downstream of Face

% FC	T Wall, °F	Heat Flux, Btu/sec-in.^{2}	Projected* $I_{s(vac)}$, sec	Throat N_f (Thermal) Zirconium Copper
20	630	8.7	440	11,000
30	530	5.7	430	40,000

*Based on Task VIII and Task IX test results with I-triplet injector.

An alternate approach to reducing the heat flux, which is being considered, is to modify the contour in an attempt to increase the throat pressure gradient and relaminarize the boundary layer. If a laminarized boundary layer could be achieved, the 0% film cooling throat heat flux could be as low as 7.5 Btu/sec-in.^{2}. The peak flux upstream of the throat is 8.7 Btu/sec-in.^{2}. Figure 35 shows the K parameter for laminarization as suggested in Reference 1.

Complete laminarization is possible when:

$$K = \frac{\mu}{\rho u}\left[\frac{1}{u}\frac{du}{dx} + 0.4\,\frac{1}{r}\frac{dr}{dx}\right] \geq 3.3 \times 10^{-6}$$

Ref 1. Moretti, P. M., Kays, W. M., "Heat Transfer to a Turbulent Boundary Layer with Varying Free Stream Velocity and Surface Temperature," Int. J. Heat and Mass Trans., Vol 8, 1965.

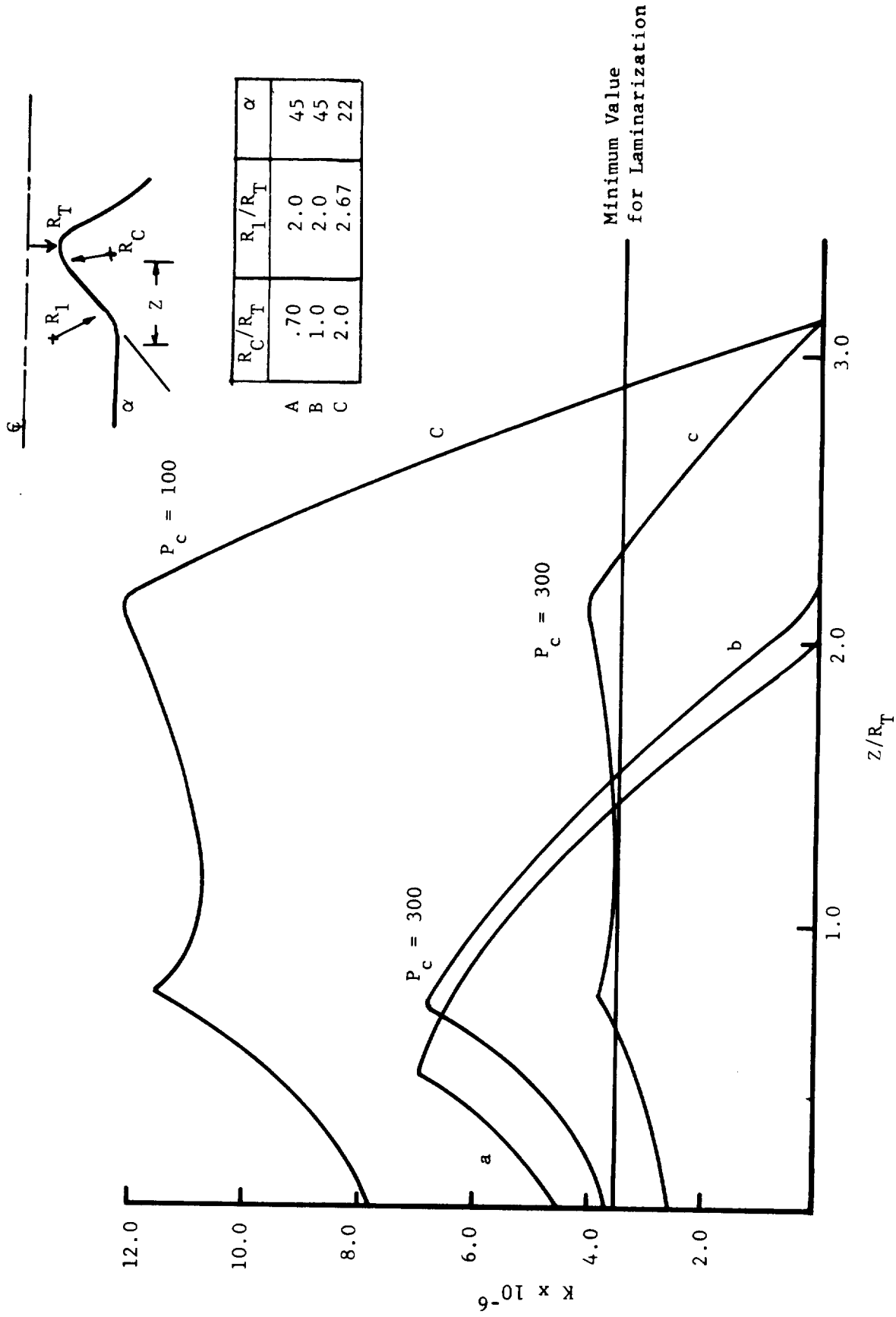

Figure 35. Criteria for Laminarization of the Regeneratively Cooled Chamber

III, B, High P_c Tasks in Redirected Program (cont.)

where μ = viscosity
ρ = density
u = free stream velocity
r = local chamber radius
x = contour length

Figure 35 shows the magnitude of the K parameter for several convergent nozzle contours at 100 and 300 psia. Contour C was employed in Task VIII testing, which demonstrated the reduced heat transfer ratio associated with a laminarized condition at 100 psia but not at 300 psia. This is consistent with the above prediction criterion, which suggests the 300 psia condition is very marginal. Modification of the contour could bring about a twofold increase in the K parameter for 300 psia operation and significantly improve the chance of a laminarized boundary layer at the throat.

The potential of employing or demonstrating this phenomenon as a means of extending chamber life and without film cooling is being evaluated.

The regeneratively cooled chamber design optimized for low temperature propellants is shown in Figure 36. Major differences between this design and Task III design are as follows:

(1) The coolant inlet manifold has been moved from area ratio 8 to area ratio 3, while the skirt film coolant injection plane is held fixed. This results in a short dump cooled section between area ratios 3.5 and 8 which serves to preheat the cold fuel used for skirt film cooling. The preheating allows higher supersonic coolant injection velocities to be achieved. Movement of the inlet manifold forward reduces the diameter of the manifold, volume of the coolant channels, and weight of the chamber.

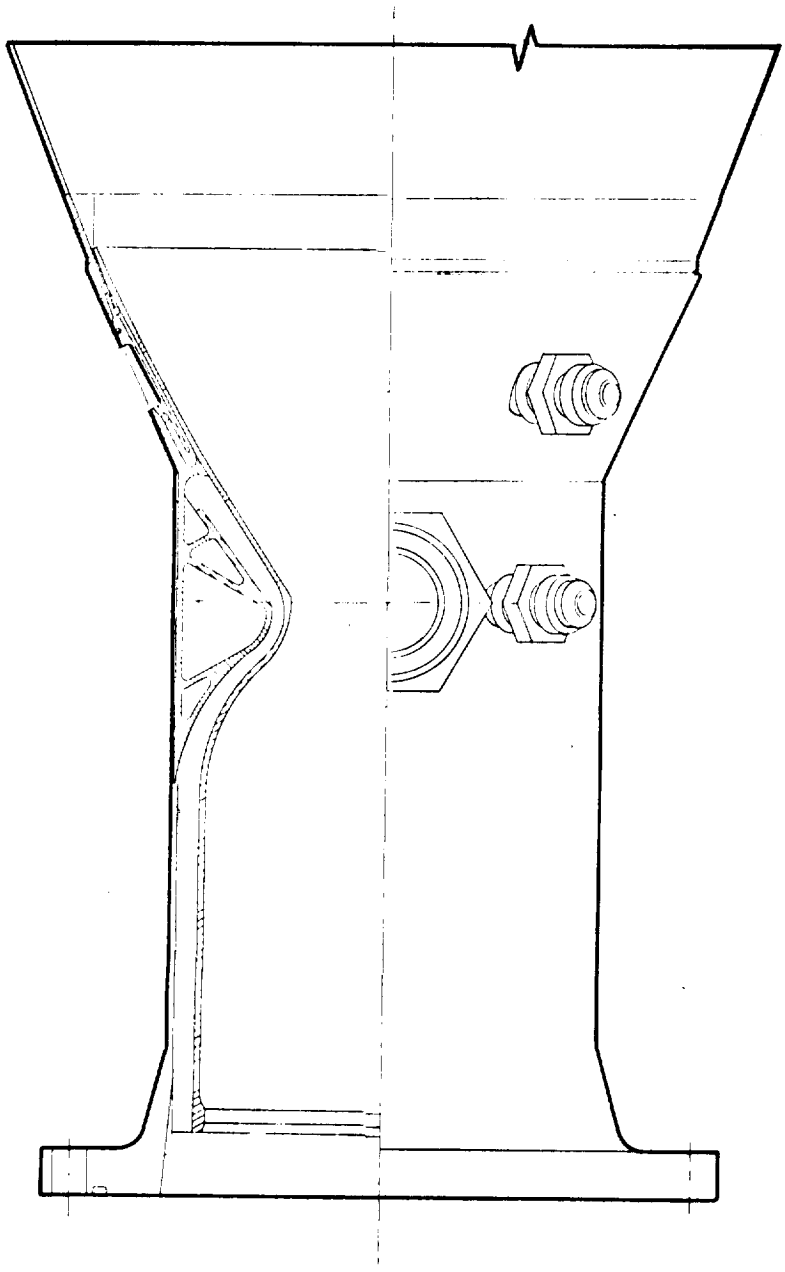

Figure 36. 3.5:1 Regeneratively Cooled Chamber Dump/Film-Cooled 40:1 Skirt

III, B, High P_c Tasks in Redirected Program (cont.)

(2) The chamber contour has been modified to produce the higher pressure gradients in the throat indicated by the laminarization analysis.

(3) The coolant channels have been modified to reduce chamber weight and coolant volume and to take advantage of the higher density low temperature coolant.

(4) The channel closeout approach has been modified to: (a) eliminate the need for machining stepped coolant channels; (b) use a photoetched, precontoured stainless steel truss in place of the hand-formed square copper wires; and (c) employ a shrunk-fit and brazed steel jacket rather than the electroformed nickel pressure vessel.

(5) Propellant and coolant are supplied through a single fuel inlet line.

Figure 37 provides a comparison of the predicted coolant velocities, heat flux profiles, and resulting chamber wall temperatures and temperature gradients for Task III and Task XXVIII regeneratively cooled chamber designs. The Task XXVIII chamber has been analyzed for two assumed limiting throat conditions: a fully turbulent boundary layer and a completely relaminarized condition for 0% film cooling. A comparison of these thermal results using theoretical thermal boundary conditions is provided in the following table. It is anticipated that the new chamber design can provide the same cyclic life without film cooling as the Task III design can provide with 20 to 30% film cooling.

Design	BL Assumption	Max Temp Gradient, °F	Max Temp, °F	Max Flux, Btu/sec-in.^{2}
Task III	Turbulent	630	970	15
Task XXVIII	Turbulent	520	640	18
	Laminar	250	420	8.7

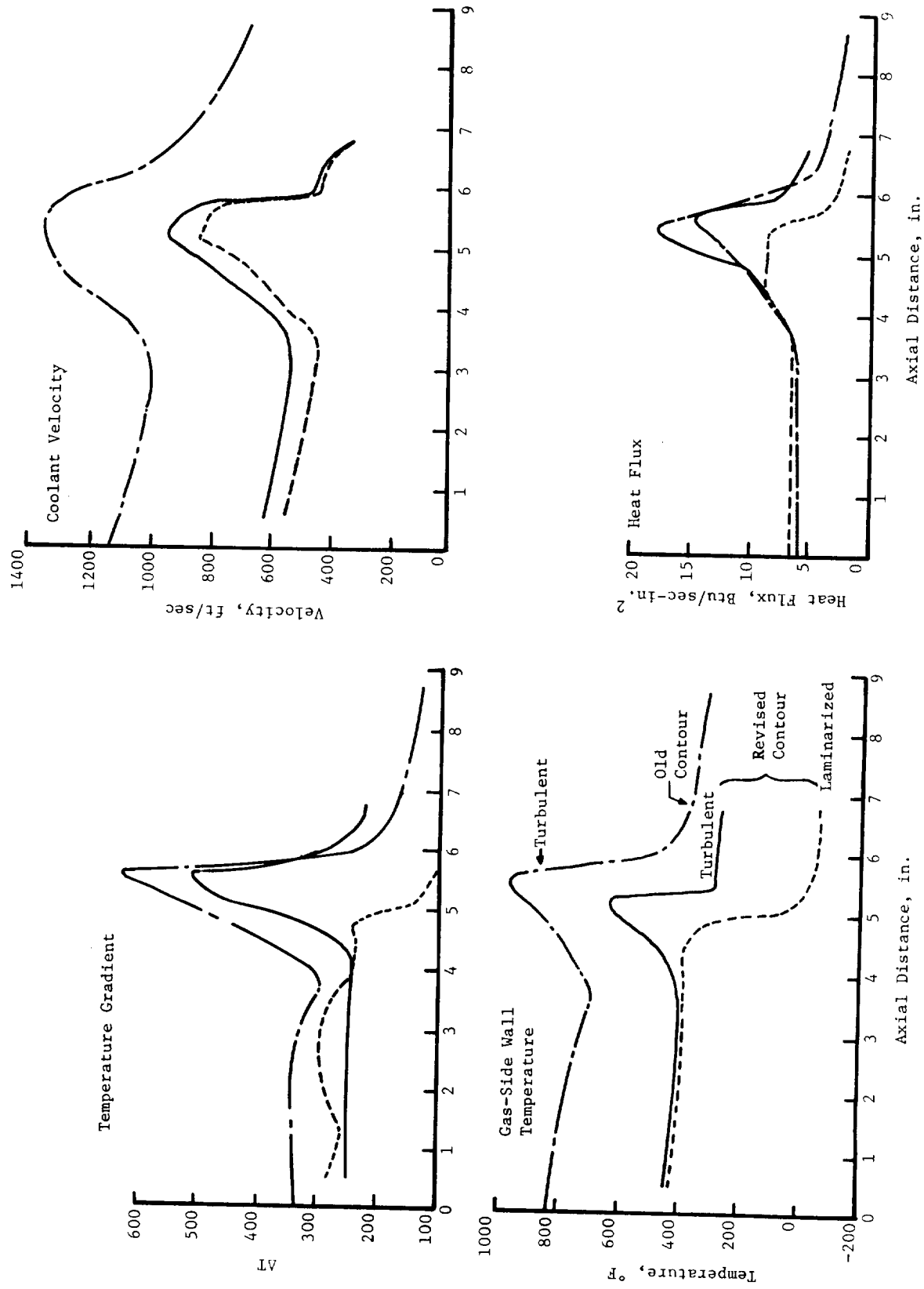

Figure 37. Regenerative Design

III, B, High P_c Tasks in Redirected Program (cont.)

7. Task XXV - Cooled Chamber Fabrication

Fabrication was initiated on the Haynes 188 throat and skirt for the new film-cooled chamber for this task.

8. Task XXVI - Injector Tests

A test plan for this activity has been prepared and submitted for NASA approval.

9. Tasks XXVII and XXVIII

No activity.

IV. WORK DURING NEXT REPORTING PERIOD

Tasks I through VIII - No activity.

Task IX - Continue cooled chamber testing and evaluate test data.

Task X - Calibrate new anemometers. Set up for pulse tests.

Task XXII - Finalize face plate pattern of injector for regeneratively cooled design and cold flow both circuits for distribution efficiency.

Task XXIII - Complete fabrication of second new low propellant temperature injector.

Task XXIV - Complete design modification efforts of chambers for low temperature propellants. Complete detailed thermal and structural and life analyses.

Task XXV - Continue fabrication of second-generation film-cooled chamber with revised coolant channels on floating manifolding. Initiate regen chamber fabrication.

Task XXVI - Conduct checkout tests on new injector.

V. PROBLEM AREAS

There are no significant technical problems. The testing is proceeding slower than planned because of test facility delays. Testing is approximately four weeks behind schedule.

FORECAST AND CONSUMPTION OF GOVERNMENT-FURNISHED PROPELLANTS

Contract NAS 3-14354

Material	Monthly Usage	Cumulative	Next Month's Requirements	Next 3 Month Requirements
LO_2 (ton)	23	23	11	180
LH_2 (lb)	0	7210	3300	14,200
LN_2 (ton)	106	417	150	375
GHe 10^3 (SCF), Bulk	0	99,100	12.5	25
GHe 10^3 (SCF), Cylinders	0	0	19	7

NATIONAL AERONAUTICS AND SPACE ADMINISTRATION

Lewis Research Center

CONTRACT PROGRESS SCHEDULE

REPORT FOR MONTH ENDING: 30 June 1971

FORM APPROVED BUDGET BUREAU NO. 104-R0007

9. NASA Use Only
a. NASA CODE
b. PROJECT MGR.
c. EVALUATION DATE
d. EXCEPTION CATEGORY
e. f. g.

1. CONTRACT TITLE: Hydrogen-Oxygen APS Engines (High P_c)

2. CONTRACTOR (Name and address): Aerojet Liquid Rocket Co., P.O. Box 13222 Sacramento, California 95813

3. CONTRACT NO.: NAS 3-14354

4. APPROVED (Contractor's Project Manager): L Thornman

PREPARATION DATE: 7-10-71

5. NASA APPROVED SCHEDULE DATE: 8-31-70

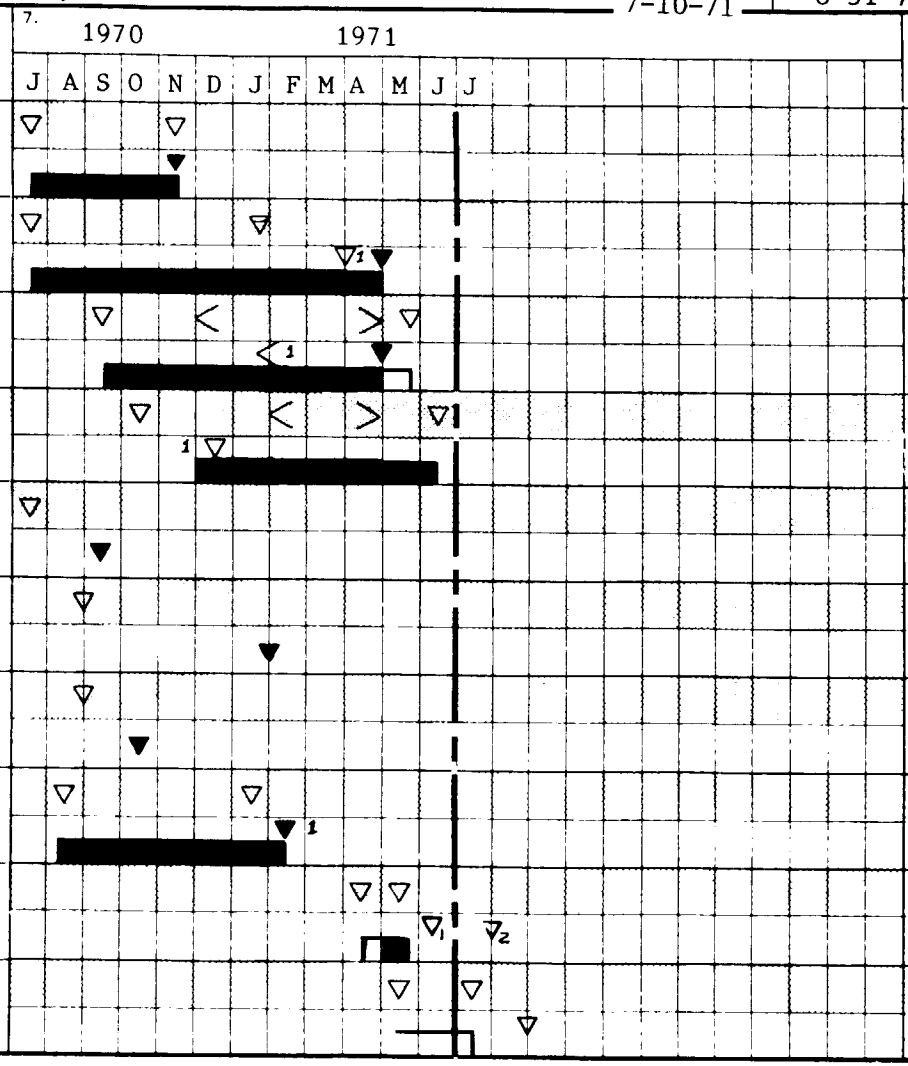

Task	6. REPORTING CATEGORY	8. TECH. OBJECTIVE % COMP.
I	Injector Analysis and Design	100
II	Injector Fabrication	100
III	Thrust Chamber Analysis and Design	100
IV	Thrust Chamber Fabrication	99
V	Ignition System Analysis and Design	100
VI	Ignition System Fabrication and Checkout	100
VII	Bipropellant Valve Preparation	100
VIII	Injector Tests	100
IX	Thrust Chamber Cooling Tests	45
X	Pulsing Tests	1

NASA-C-63 (Rev 1-68)

NASA APPROVED SCHEDULE

CONTRACTOR'S WORKING SCHEDULE

NATIONAL AERONAUTICS AND SPACE ADMINISTRATION

Lewis Research Center

CONTRACT PROGRESS SCHEDULE

REPORT FOR MONTH ENDING: 30 June 1971

FORM APPROVED. BUDGET BUREAU NO. 104-R0007

9. NASA Use Only
a. NASA CODE
b. PROJECT MGR.
c. EVALUATION DATE
d. EXCEPTION CATEGORY

1. CONTRACT TITLE: Hydrogen-Oxygen APS Engines (Low P_c)

2. CONTRACTOR (Name and address): Aerojet Liquid Rocket Company, P.O. Box 13222 Sacramento, California

3. CONTRACT NO.: NAS 3-14354 Amendment I

4. APPROVED (Contractor's Project Manager): A A Dare — PREPARATION DATE: 7-10-71

5. NASA APPROVED SCHEDULE DATE: 8-31-70

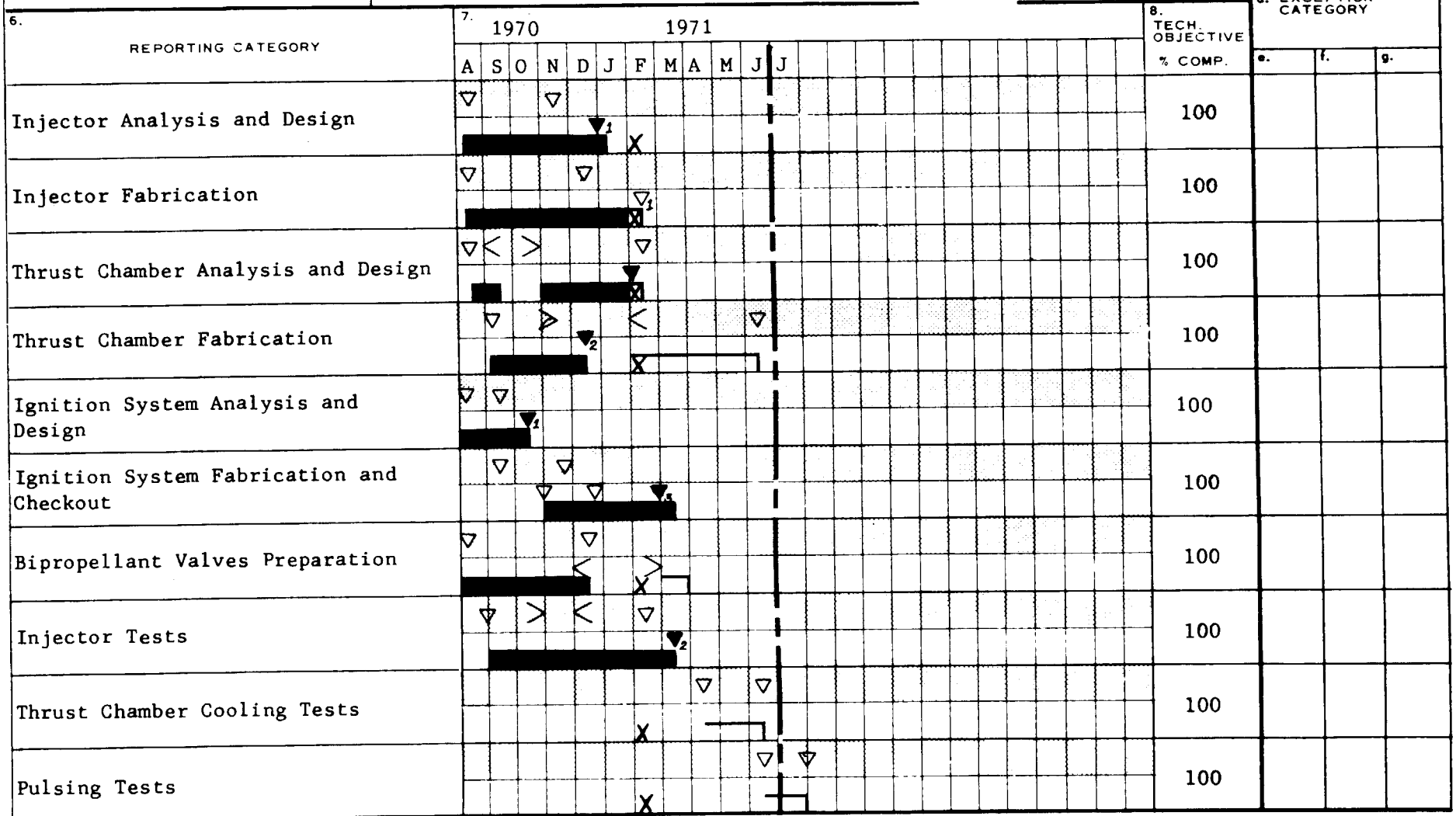

NASA-C-63 (Rev. 1-68)

NASA APPROVED SCHEDULE

CONTRACTOR'S WORKING SCHEDULE

X Indicates activities halted by stop work order dated 11 February 1971.

NATIONAL AERONAUTICS AND SPACE ADMINISTRATION

Lewis Research Center

CONTRACT PROGRESS SCHEDULE

REPORT FOR MONTH ENDING: 30 June 1971

FORM APPROVED. BUDGET BUREAU NO. 104-R0007

9. NASA Use Only
a. NASA CODE
b. PROJECT MGR.
c. EVALUATION DATE
d. EXCEPTION CATEGORY

1. CONTRACT TITLE: Hydrogen-Oxygen APS Engines

2. CONTRACTOR (Name and address): Aerojet Liquid Rocket Company, P.O. Box 13222 Sacramento, California 95813

3. CONTRACT NO.: NAS 3-14354

4. APPROVED (Contractor's Project Manager): R J Lo Bert

PREPARATION DATE: 7-10-71

5. NASA APPROVED SCHEDULE DATE: 8-31-70

Task: XXI

6. REPORTING CATEGORY	8. TECH. OBJECTIVE % COMP.	e.	f.	g.
Program Plan and Test Plans				
High P_c	71			
Low P_c	100			
Monthly Reports	72			
Quarterly Reports	100			
Final Report Draft	25			

7. 1970 J A S O N D — 1971 J F M A M J J A S O N

NASA-C-63 (Rev. 1-68)

NASA APPROVED SCHEDULE

CONTRACTOR'S WORKING SCHEDULE

NATIONAL AERONAUTICS AND SPACE ADMINISTRATION
Lewis Research Center

CONTRACT PROGRESS SCHEDULE

REPORT FOR MONTH ENDING: 30 June 1971

FORM APPROVED. BUDGET BUREAU NO. 104-R0007

9. NASA Use Only
a. NASA CODE
b. PROJECT MGR.
c. EVALUATION DATE
d. EXCEPTION CATEGORY

1. CONTRACT TITLE: Hydrogen-Oxygen APS Engines (High P_c)

2. CONTRACTOR (Name and address): Aerojet Liquid Rocket Co., P.O. Box 13222 Sacramento, California 95813

3. CONTRACT NO.: NAS 3-14354

4. APPROVED (Contractor's Project Manager): L Schoenman

PREPARATION DATE: 7-10-71

5. NASA APPROVED SCHEDULE DATE

Task	6. REPORTING CATEGORY For Low Temperature Propellants	8. TECH OBJECTIVE % COMP.	e.	f.	g.
XXII	Injector Analysis & Design	85			
XXIII	Injector Fabrication	75			
XXIV	Thrust Chamber Analysis and Design	75			
XXV	Thrust Chamber Fabrication	5			
XXVI	Injector Checkout Tests	2			
XXVII	Cooled Chamber Tests	0			
XXVIII	Pulse Tests	0			

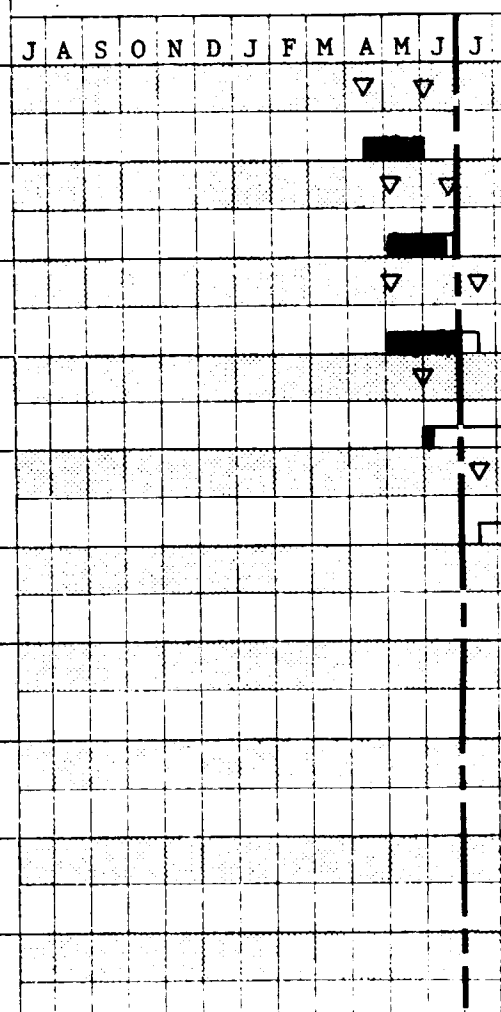

NASA C-62 (Rev. 1-65)

NASA APPROVED SCHEDULE
CONTRACTOR'S WORKING SCHEDULE